ANALYSIS AND OPERATION OF A MICROGRID WITH PHOTOVOLTAIC SOURCES

A Thesis
Presented to
The Academic Faculty

By

Juan C. Lazarte

In Partial Fulfillment
Of the Requirements for the Degree
Master of Science in Electrical and Computer Engineering

Georgia Institute of Technology

May 2018

ANALYSIS AND OPERATION OF A MICROGRID WITH PHOTOVOLTAIC SOURCES

Approved by:

Dr. A.P. Sakis Meliopoulos, Advisor
School of Electrical and Computer Engineering
Georgia Institute of Technology

Dr. Santiago C. Grijalva
School of Electrical and Computer Engineering
Georgia Institute of Technology

Dr. Maryam Saeedifard,
School of Electrical and Computer Engineering
Georgia Institute of Technology

Date Approved: April 2018

To God, who continues to guide me and give me strength throughout all challenges.

To my dear parents, who taught me to believe in myself.

To my good friends, who were there for me in the most difficult moments.

ACKNOWLEDGMENTS

I remember coming to Georgia Tech in the fall of 2016. After a few personal experiences of failures and successes, I knew I was ready for the challenge, but still had the fear of future struggles. This, my first time living abroad, has been a process of continuous learning, filled with remarkable experiences and everlasting memories. It has also been the best proof that constant effort and trust in God's will makes everything possible.

I especially want to recognize my Advisor, Professor A.P. "Sakis" Meliopoulos for his patience and for giving me the chance to develop my skills under his guidance.

This experience would not have been the same without the support of the Fulbright Network. Thank you for placing your trust in me, and for the opportunity to apply my knowledge to make the world a better place. Learning to use technologies that can be applied in developing regions is my commitment to my home country of Peru, and to my fellow colleagues around the globe.

Ad majorem Dei gloriam

For the greater glory of God.

TABLE OF CONTENTS

LIST OF TABLES

LIST OF FIGURES

LIST OF ABBREVIATIONS

PV	Photovoltaic
DC	Direct current
AC	Alternating current
DG	Distributed generation
DER, DR	Distributed energy resources
ESS	Energy storage systems
p.u.	Per-unit system
RMS	Root-mean-square
EPQ	Electric power quality
THD	Total harmonic distortion
PDF	Power distortion factor
QDF	Reactive power distortion factor
ADF	Apparent power distortion factor
TG	Turbine generator
PCC	Point of common coupling
EPS	Electric power system
ITE	Information technology equipment
MAX	Open measurement & automation explorer
NI	National instruments
DAQ	Data acquisition
TF, TRAFO	Transformer
CT	Current transformer
PSCSV	Power sentinel CSV
PMU	Phasor measurement unit
FFT	Fast Fourier transform
UTC	Coordinated universal time

SUMMARY

The present work focuses on the study of a physical module implemented in the Power Systems Control and Operation Laboratory at the Georgia Institute of Technology. The system, which is referred to as the microgrid, consists of a solar generation unit, a central inverter, power electronics, measuring devices, data acquisition systems, and a mainly resistive load. The microgrid operates by connecting to the bulk power grid. The objective of this research is to understand the principles of the operation of a microgrid and to perform its electric power quality assessment. Part of the work involves describing and configuring the settings for proper operation of the microgrid and the data acquisition systems. The main contribution of this master's thesis is to develop methods to perform power quality assessment of this specific system in accordance with the relevant quality standards: the IEEE Std. 519, "IEEE Recommended Practice for Harmonic Control in Electric Power Systems", and the IEEE Std. 1547, "IEEE Standard for Interconnecting Distributed Resources with Electric Power Systems". The results and conclusions are all based on real measurements and are used to discuss simple design criteria to evaluate how different distributed energy resources would impact the local power system.

CHAPTER 1: INTRODUCTION

The traditional bulk power grid follows a design and architecture based on matching the electric power generation to a given energy consumption continuously. The grid itself is a complex system with fast and slow dynamics. The existent power infrastructure includes components at the end of their operational lifetime, which are often not as efficient as new technologies emerging in the market. Only in transmission and distribution, electricity losses in the power grid represent an average of 5% of the total energy transmitted and distributed in the United States [1]. In addition, if we consider the capabilities of the power devices that are not being used, the capacity of the whole power system is actually much higher as long as it is properly controlled and managed.

Some of the new concepts that are recently being applied to the grid can be found in new electronic devices with more capabilities than legacy technologies. For example, in different grid operation and automatic control schemes, and in more efficient ways to generate, transport and store energy. These efforts challenge many concepts applied in the traditional power system. Rather than focusing on the reduction of losses and accommodations of new technologies, new applications introduce a series of changes with the potential to achieve better efficiency in both the way energy is generated and consumed. Then, the concept of a “smart grid” is used to refer to a power system that takes these aspects into consideration for its architecture and design.

With the massive introduction of power electronics in the grid, new technical challenges have been introduced to the power grid. Some of the most noticeable difficulties are: impact of distributed generation on the existing distribution network; need to reduce transient voltage variations and harmonic distortion in the new variable, changing grid.

This master's thesis represents an effort to better understand the impact of a market application (a solar generation unit) in the local power grid as a necessary step to implement similar technologies at a higher scale. The goals of this project are to perform the power quality assessment of the energy coming from the module, as well as to set up the conditions for a later analysis of the impact of the interconnection of this module with the utility grid.

CHAPTER 2: LITERATURE SURVEY

2.1. Basic concepts of operation of a PV module

2.1.1. Solar irradiance as a dynamic space-time function

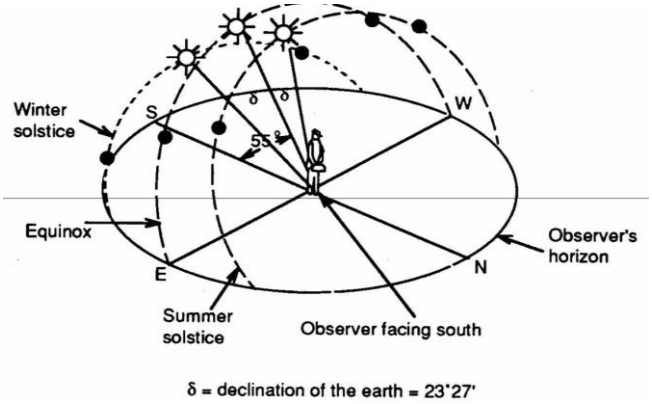

Figure 2.1: Change in the sun position over the year. [2]

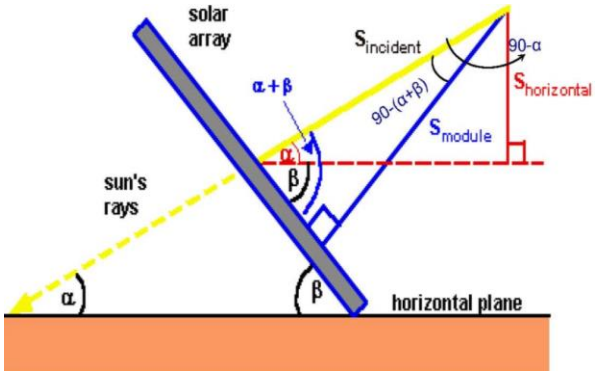

Figure 2.2: Direct solar irradiation on a tilted surface. [3]

Photovoltaics are dynamic systems relying on the solar irradiance to produce electricity. As the position of the sun changes throughout the year (see Figure 2.1), so

does the amount of radiation that faces any location on earth. However, such changes also depend on other factors: latitude (α), declination for a day, hour angle (ω). A simple, didactic model used in the Solar Cell course by Dr. A. Rohatgi at Georgia Tech relates the mentioned factors following the relationship:

$$\boldsymbol{Sin\,\alpha = cos\,\varphi * cos\delta * cos\omega + sin\varphi * sin\delta} \qquad (1)$$

The amount of solar power irradiated directly on a tilted surface follows the formula:

$$S_\beta = S * \frac{\sin(\alpha+\beta)}{sin\,\alpha} \text{ and } D+S_\beta = G_\beta \qquad (2)$$

This means there is an amount of the solar radiation G_β that does not change with the panel tilt (β), which is called "diffuse radiation" D. For a clear day, in general, the value of D can be taken as the 10% of the direct solar radiation S_β. Due to the change in the position of the sun throughout the day, the power output of a solar panel will change, even if its efficiency η was constant and so were the atmospheric conditions.

2.1.2. Solar cells' structure and parameters of operation

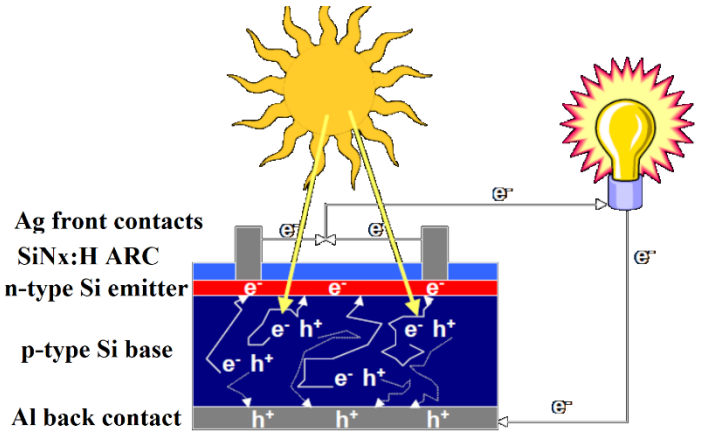

Figure 2.3: Basic components of a silicon-based solar cell. [4]

The basic components of most solar cells are semiconductor materials, whose properties vary with their composition. Semiconductors doped with elements that can donate electrons to silicon, such as those from the VI group of the periodic table, have an increased number of electrons in the conduction band. These semiconductors are known as n-type materials. Semiconductors doped with elements that can accept electrons from Silicon, such as those from the III group of the periodic table, are known as p-type materials. The electronic asymmetry within a p-n junction encourages the flow of electrons from the n-type region to the p-type region and the flow of holes in the opposite direction, generating current.

Solar energy in the form of photons is absorbed in a semiconductor, which allows the generation of electron-hole pairs. To generate electricity, they must travel all the way towards from their respective regions to the electric grid and live long enough by avoiding recombination within the solar cell. When electrons get to the p-n junction, they are separated by an electric field and collected by metal contacts thus providing electricity to the PV System.

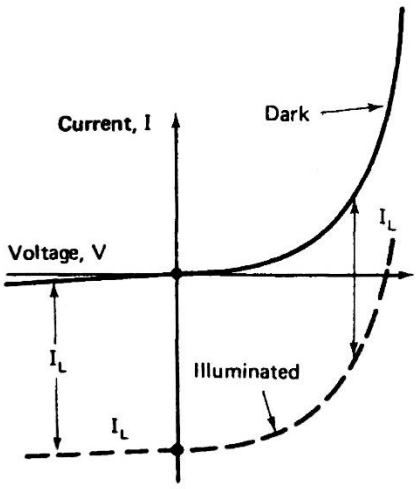

Figure 2.4: VI curve of a solar cell under forward voltage bias. [5]

The parameters used to characterize the terminal properties of a solar cell are the short circuit current *Isc*, the open-circuit voltage *Voc* and the fill factor *FF*. The fill factor measures how square the output characteristics of a solar cell are (see image 4, above) and it is defined as:

$$FF = V_{mp}I_{mp}/V_{oc}I_{sc} \qquad (3)$$

Where V_{mp} and I_{mp} are the voltage and current of the cell in which the maximum output power is achieved. Since the characteristics of the solar cell change with a series of factors (temperature and solar irradiance are just some of them), it is convenient for systems with large power capacity to have a device that always tracks the maximum power point of the cell to achieve its maximum efficiency.

2.1.3. Components of a simple PV system

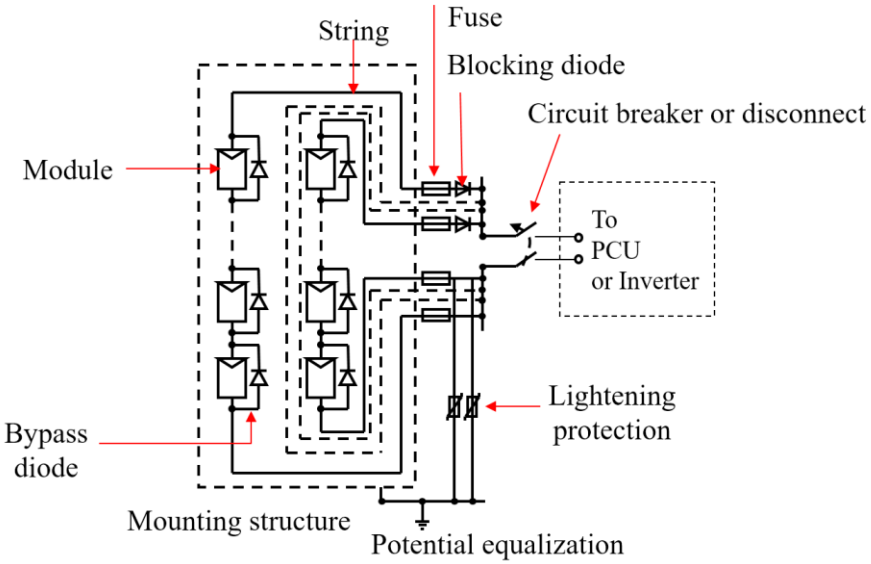

Figure 2.5: Basic components of a PV system. [4]

A PV generation system comprises different components. Basically, solar cells can be connected in series to add up their voltage, and in parallel to add up the current output. A PV system also contains bypass diodes between strings to prevent shadowed or faulted cells affect the overall power rating of the panel. Without bypass diodes, strings of cells with lower outputs would be forced to produce the same current than healthy cells connected in series. This would drive faulty cells to the reverse bias mode, and therefore the current flowing in the opposite direction would generate hot spots in them. Other protection devices and breakers are also included in a PV system.

2.1.4. Modes of operation of a PV system

The main difference between a grid-connected and a standalone PV system is autonomy. In order to achieve more reliability and provide good energy quality, a standalone system must have a storage system or must be oversized. In the case of batteries, a charge controller should be included to prevent surpassing limits that may damage them. One or several backup generators can be included for increased reliability. In case of grid-connected systems, no storage is necessary as it can take energy from the grid when no generation is available. To provide energy to the grid or feed AC loads, it is necessary to count on inverters since the PV system's output is DC.

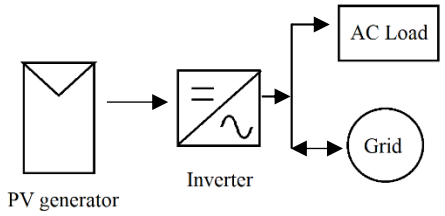

Figure 2.6: Diagram of a grid-connected PV system.

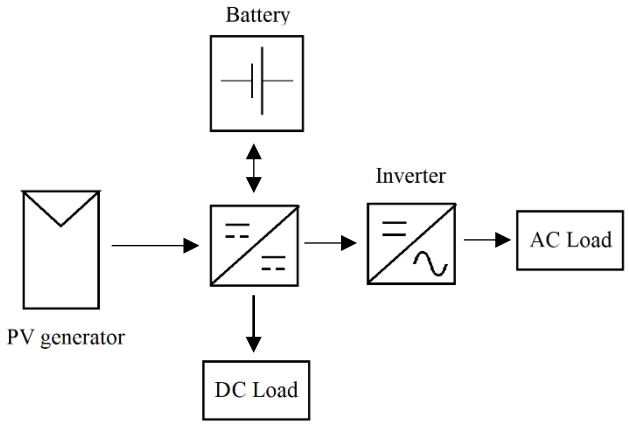

Figure 2.7: Diagram of a standalone PV system.

2.2. Challenges to the integration of distributed generation (DG).

The authors Peças Lopes et al. have identified in [6] the following effects that the integration of distributed energy resources into the bulk grid may have:

2.2.1. Voltage rise effect [7]

Power flow in distribution systems is traditionally unidirectional from the main power generator to the load. However, due to a large penetration of DG into the distribution system, voltage increases in several points of the system and could result in power flow in different directions. The new system design must consider the power that may be exported back to the main grid, and it should ensure that the system (especially the protection system) is capable to operate with "reverse" power flow. These factors may limit the amount of additional DG capacity that can be connected to the traditional distribution network.

2.2.2. Problems in the final power quality [8]

- Transient voltage variations are a result of relatively large current changes. Typically, such currents are generated during connection and disconnection of generators, but they can be limited by a good design of the distributed generation plants. The use of controllable inverters can help mitigate this issue.

- Harmonic distortion of the grid's voltage is a result of poorly designed electronic interfaces within a distributed generation plant. As a consequence, there can be an injection of harmonic currents leading to unacceptable voltage distortions. A serious concern is that the capacitance and reactance of the microgrid could produce great power distortion if the injected harmonics work close enough to resonant frequencies of the local power system.

2.2.3. Fault protection design

Besides the default protection of the generation equipment from internal faults, the following topics must be considered:

- Impact of DG on the existing distribution system.
- Protection of the faulted distribution network from fault currents supplied by the DG.
- Anti-islanding protection: To stop or change the operation of the DG when there is an outage in the main power grid.

2.2.4.Stability analysis

Traditionally, distribution networks design does not consider issues of stability. The legacy distribution network was passive and remained stable provided the transmission network itself was stable. Stability is hardly considered when assessing renewable distributed generation schemes. However, the contribution of DG becomes greater and might change the way the distribution system is analyzed. The areas that need

to be considered include transient as well as long-term dynamic stability and voltage collapse.

2.3. State of the art in microgrids research

2.3.1. Microgrid definition and characteristics [9]

The U.S. Department of Energy Microgrid Exchange Group defines microgrid as "a group of interconnected loads and distributed energy resources (DERs) within clearly defined electrical boundaries that acts as a single controllable entity with respect to the grid" [10]. Other definitions can also be found, but most of them have in common the following characteristics:

- They have clearly defined electrical boundaries.
- There must be a master controller that operates distributed energy resources (DER) and loads as a single controllable entity.
- The installed generation capacity must exceed the peak critical load. Thus, it could be disconnected from the utility grid (islanded mode) and supply local critical loads without interruption.

2.3.2. Main components of a microgrid

- Loads, commonly categorized into two types:
  - Fixed loads: cannot be altered and must be satisfied under normal operating conditions.

    - Flexible loads: responsive to control signals. They could be curtailable (reduced) or deferred (shifted).
- Distributed generators, fitting in two categories:
    - Dispatchable units: can be controlled by the microgrid's master controller.
    - Non-dispatchable units: whose input source is exogenous, and their operation is desired to be at maximum power tracking. Typically, solar and wind generators. Because of their volatile and intermittent nature, the forecast error could impact the operation of the grid. That is why they are usually reinforced with an electric storage system.
- Energy storage systems (ESS). They usually have two functions:
    - To guarantee the adequacy of the microgrid's power generation.
    - To store for market purposes, which enables the sale of the energy to the main grid when the price is high.

2.3.3. Some recent studies in microgrid technologies

The authors S. Parhizi, H. Lotfi, A. Khodaei, S. Bahrramirad have compiled a useful source of over 30 research articles about distributed generation and microgrids in [11]. For purposes of this thesis, we are presenting a compilation of those most related to our project.

- Distributed generation
    - The study in [12] analyses the reduction of energy balance fluctuations in a small-scale microgrid by optimizing a diverse set of renewable energy generation technologies.

- The study in [13] proposes a ‘‘provisional microgrid’’, one without islanding capability, in order to facilitate the integration of intermittent energy sources to the utility grid without relying only on them.

- Energy storage systems (ESS)
  - The study in [14] proposes an algorithm for microgrids involving ESS to manage their devices in real-time; to mitigate pulsed loads effects on the system performance.
  - The study in [15] shows that ESS applied in microgrids can perform the task of active power balancing and voltage regulation at the same time.
- Reliability assessment
  - In [16], metrics and procedures are proposed for the reliability assessment of islanded microgrids.
  - The study in [17] considers the probabilistic behavior of solar and wind power using reduced data inputs as compared to a Monte Carlo approach for the reliability calculations.
- Reliability improvement
  - The study in [18] proposes a dispatching strategy based on limiting the risk in operation, rather than the worst-case dispatch by using real-time information about supply and demand.
  - The study in [19] applies the control of charge and discharge of electric vehicles that helps relieve the grid load during peak hours.
- Resiliency (recovery against high-impact faults)

- The study in [20] proposes a decentralized multi-agent control for distributed microgrids, allowing agents to transition from normal to an emergency operation and back when the harmful conditions are over.
- The study in [21] proposes a reconfigurable system design to facilitate the realization of fault prevention, detection, and mitigation at various levels. It includes distributed state estimation that is supported by control theoretic security solutions.

- Power quality compensation
  - The study in [22] proposes a group of grid-interfacing system topologies to interface local microgrids to the utility grid or between them to enhance the overall voltage quality.
  - The study in [23] proposes a power quality compensator to be used with individual DGs in a microgrid, using optimally controlled inverters to enhance the power quality and currents flowing between the microgrid and the utility grid.
- Harmonic filtering and mitigation
  - The study in [24] applies a cooperative strategy for the interface converters of DGs, where all the DG converters evenly share the overall harmonic filtering workload.
  - The study in [25] shows how to change a small grid into an autonomous microgrid by implementing additional control and ESS. This study is especially focused on the harmonic problem from the interaction between grid components and solar inverters.

2.4. Summary of power quality theory

2.4.1. Classification of power system disturbances

Table 2.1: Types of power system disturbances. [26]

Disturbance type	Short definition	Index relevant to this project
Interruption	Voltage magnitude is zero	None
Under voltage	Voltage magnitude below nominal value for more than 1 min	Voltage in p.u.
Over voltage	Voltage above below nominal value for more than 1 min	Voltage in p.u.
Voltage sag	Reduction in RMS voltage over a range of 0.1-0.9 p.u. for a duration greater than 10ms or 0.5 cycles but less than 1min	Voltage in p.u.
Voltage swell	Increase in RMS voltage over a range of 1.1-1.8 p.u. for a duration greater than 10ms or 0.5 but less than 1min	Voltage in p.u.
Voltage fluctuations - Flicker	Visual effect of frequency variation of voltage in a system	Flicker factor
Voltage or current unbalance	Deviation in the magnitude of voltage/current of any of the three phases	N/A
Ringing waves	Transient condition which decays gradually	THD, IHD, Crest factor
Outage	Power interruption for not exceeding 60s duration	None
Transient	Sudden rise of a signal	THD, IHD, Crest factor
Harmonics	Non-sinusoidal waveforms	THD, IHD, Crest factor

2.4.2.Power quality parameters

Table 2.2: Electric power quality parameters. [26]

EPQ parameter	Definition
Total Voltage Harmonic Distortion (THD_V)	$\left(\sqrt{\sum_{n=2}^{n=\infty} V_n^2}\right) / V_1$
Total Current Harmonic Distortion (THD_I)	$\left(\sqrt{\sum_{n=2}^{n=\infty} I_n^2}\right) / I_1$
Active power distortion factor	$PDF = \frac{P_H}{P_1} \times 100\%$
Reactive power distortion factor	$QDF = \frac{Q_H}{Q_1} \times 100\%$
Apparent power distortion factor	$ADF = \frac{A_H}{A_1} \times 100\%$
Flicker factor	$\Delta V / \lvert V \rvert$
Crest factor	V_{peak} / V_{RMS}
PQ index	$\left[\left\lvert \frac{\mathrm{V} - 100\%}{V_{CBEMA}(t) - 100\%} \right\rvert\right] .100\%$

2.4.3. Effect of Harmonics in electrical components

Table 2.3: Effects of harmonics in electrical components. [27]

Name of component	Effects of harmonics
Generator	Production of pulsating or oscillating torques which involve torsional oscillations of rotor elements of TG set and rotor heating
Motor	Stator and rotor copper losses increase due to harmonic current flow, leakage flux created by harmonic currents causes additional stator and rotor losses, core loss increases due to harmonic voltages and positive sequence harmonics develop shaft torques that aid shaft rotations whereas negative sequence opposes it
Transformer	Stray losses increase due tom harmonic current flow, hysteresis losses increase, due to presence of high frequency harmonics resonance may occur between winding inductance and line capacitance
Relaying	Mal-tripping may occur due to presence of harmonics which affects the time delay characteristics
Switchgear	Due to predominance of skin and proximity effects at higher frequencies, bus-bars behave like cables and transient recovery voltage changes which affect the operation of blow-out coils
Capacitor	Due to presence of harmonics, reactive power increases, dielectric losses increase causing additional heating and resonance and overvoltage may occur, resulting in reduced life
Cables	Due to increased skin and proximity effects at higher frequencies, additional heating occurs, R_{ac} increases and ac copper loss increases
Consumer equipment	Life and efficiency reduce drastically
Communication circuits	Noise creeps in transmitted signals

2.5. Relevant American standards in power quality

2.5.1. IEEE-591. Recommended Practice and Requirements for Harmonic Control in Electric Power Systems [28]

- Certifications: any instrument used should comply with the general specifications of IEC 61000-4-7 and IEC 61000-4-30 for harmonic measurements.
- Window width: the width of the measurement window should be 12 cycles (approximately 200 ms) for 60 Hz power systems (10 cycles for 50 Hz power systems).
- Resolution: spectral components will be available every 5 Hz (e.g., 0, 5, 10…50, 55, 60, 65, 70, … Hz).
- Grouping: a harmonic component magnitude is considered to be the value at a center frequency combined with the two adjacent 5 Hz bin values. See image 2.8.
- Types of measurements:

Very short time harmonics: Assessed over a 3s span, which corresponds to an aggregation of 15 consecutive 12-cycle windows for 60Hz.	$F_{n,vs} = \sqrt[2]{\frac{1}{15}\sum_{i=1}^{15} F_{n,i}^2}$ (4)
Short time harmonic values: assessed over a 10-minute interval, corresponding to an aggregation of 200 consecutive very short time values for a specific frequency component.	$F_{n,sh} = \sqrt[2]{\frac{1}{200}\sum_{i=1}^{200} F_{(n,vs),i}^2}$ (5)
F represents RMS voltage (*V*) or current (*I*), *n* represents the harmonic order, and *i* is a simple counter.	

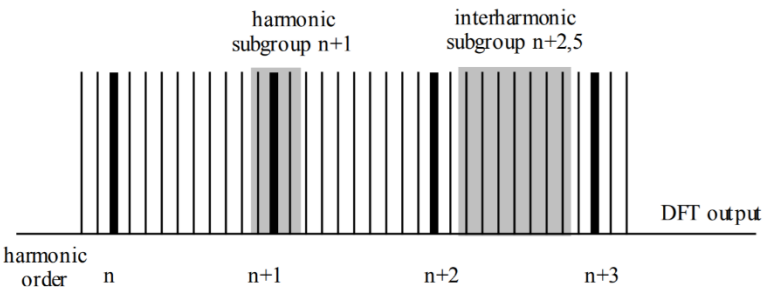

Figure 2.8: Harmonic and inter-harmonic grouping. [29]

Tolerance limits

- For the case of voltages, the IEEE Std. 519 establishes the limits for measurements evaluated at the point of common coupling (PCC). The general limits are established in table 2.4.
- At the PCC, system owners or operators should limit line-to-neutral voltage harmonics as follows:
  - Daily 99th percentile very short time (3 s) values should be less than 1.5 times the values given in the tables.
  - Weekly 95th percentile short time (10 min) values should be less than the values given in the tables.

Table 2.4: Voltage distortion limits for Power Systems. [28]

Bus voltage V at PCC	Individual harmonic (%)	Total harmonic distortion THD (%)
$V \leq 1.0$ kV	5.0	8.0
1 kV < $V \leq 69$ kV	3.0	5.0
69 kV < $V \leq 161$ kV	1.5	2.5
161 kV < V	1.0	1.5[a]

[a]High-voltage systems can have up to 2.0% THD where the cause is an HVDC terminal whose effects will have attenuated at points in the network where future users may be connected.

- Similarly, Table 2.5 shows the tolerable limits for harmonic current injection, measured as a percentage of the maximum load current at the PCC:

Table 2.5: Current distortion limits for power systems. [28]

Maximum harmonic current distortion in percent of I_L						
Individual harmonic order (odd harmonics)[a, b]						
I_{SC}/I_L	$3 \le h < 11$	$11 \le h < 17$	$17 \le h < 23$	$23 \le h < 35$	$35 \le h \le 50$	TDD
< 20[c]	4.0	2.0	1.5	0.6	0.3	5.0
$20 < 50$	7.0	3.5	2.5	1.0	0.5	8.0
$50 < 100$	10.0	4.5	4.0	1.5	0.7	12.0
$100 < 1000$	12.0	5.5	5.0	2.0	1.0	15.0
> 1000	15.0	7.0	6.0	2.5	1.4	20.0

[a]Even harmonics are limited to 25% of the odd harmonic limits above.

[b]Current distortions that result in a dc offset, e.g., half-wave converters, are not allowed.

[c]All power generation equipment is limited to these values of current distortion, regardless of actual I_{sc}/I_L.

where

I_{sc} = maximum short-circuit current at PCC

I_L = maximum demand load current (fundamental frequency component) at the PCC under normal load operating conditions

2.5.2. IEEE 1547. The IEEE Standard for Interconnecting Distributed Resources with Electric Power Systems [30]

Relevant definitions:

- Point of common coupling (PCC): The point where a local electrical power system (EPS) is connected to an area EPS.
- Point of distributed resources (DR) Connection: The point where a DR unit is electrically connected in an EPS.

General requirements

- Voltage regulation:
  - The DR shall not actively regulate the voltage at the PCC

- The DR shall not cause the area EPS service at other local EPSs to go outside the requirements of ANSI C84.1, range 1 (see section 2.5.3)

- Response to abnormal conditions:

  Voltage:

  When any voltage is in the range given in Table 1, the DR shall cease to energize the area EPS within the clearing time as indicated.

Table 2.6: Voltage operation limits for DER. [30]

Default settings[a]		
Voltage range (% of base voltage[b])	Clearing time (s)	Clearing time: adjustable up to and including (s)
V < 45	0.16	0.16
45 ≤ V < 60	1	11
60 ≤ V < 88	2	21
110 < V < 120	1	13
V ≥ 120	0.16	0.16

[a] Under mutual agreement between the EPS and DR operators, other static or dynamic voltage and clearing time trip settings shall be permitted

[b] Base voltages are the nominal system voltages stated in ANSI C84.1-2011, Table 1.

The voltages shall be detected at either the PCC or the point of DR if the aggregate capacity of DR systems connected to a single PCC is less or equal to 30 kW, among other conditions.

- Power quality

  DC Injection: It is limited to 0.5% of the full rated output current at the point of DR connection.

Harmonics: for balanced loads, harmonic current injection into the area EPS at the PCC shall not exceed the following limits:

Table 2.7: Current harmonics injection limits. [30]

Individual harmonic order h (odd harmonics)[b]	h < 11	11 ≤ h < 17	17 ≤ h < 23	23 ≤ h < 35	35 ≤ h	Total demand distortion (TDD)
Percent (%)	4.0	2.0	1.5	0.6	0.3	5.0

[a] I = the greater of the Local EPS maximum load current integrated demand (15 or 30 minutes) without the DR unit, or the DR unit rated current capacity (transformed to the PCC when a transformer exists between the DR unit and the PCC).
[b]Even harmonics are limited to 25% of the odd harmonic limits above.

Harmonic distortion: The DR shall be operated with a predominantly inductive voltage source with a Short Circuit current of not less than 20 times the DR rated current. The individual harmonic distortion and total rated-current distortion of the output current shall be measured from the first 40 harmonics.

2.5.3. ANSI C84.1. American National Standard for Electric Power Systems and Equipment [31]

- The requirements of this standard differ in two categories: Range A for nominal conditions and Range B for short and infrequent conditions. See tolerances below.
- The National Electrical Code allows up to a 5% voltage drop in distribution systems. This is, between 114 and 126 for a 120V system. Out of that, there

can be up to a <3% voltage drop in a feeder and an additional <3% drop in individual branch circuits.

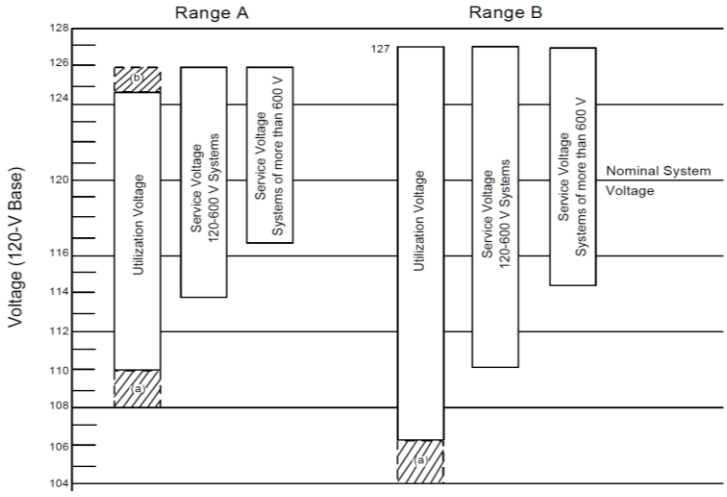

(a) These shaded portions of the ranges do not apply to circuits supplying lighting loads.
(b) This shaded portion of the range does not apply to 120-600-volt systems.

Figure 2.9: Voltage limit ranges, ANSI C84.1 [32]

a. ITI (CBEMA) acceptability curve:

- Equipment manufacturers usually specify the maximum voltage deviations within which their equipment can operate. A representative envelope curve for tolerances of equipment is the ITE acceptability curve.
- The normal functional state of most information technology equipment (ITE) would not be expected to operate in the “no damage” region, but no harm should result.
- If the ITE is subjected to the prohibited region, damage may result.

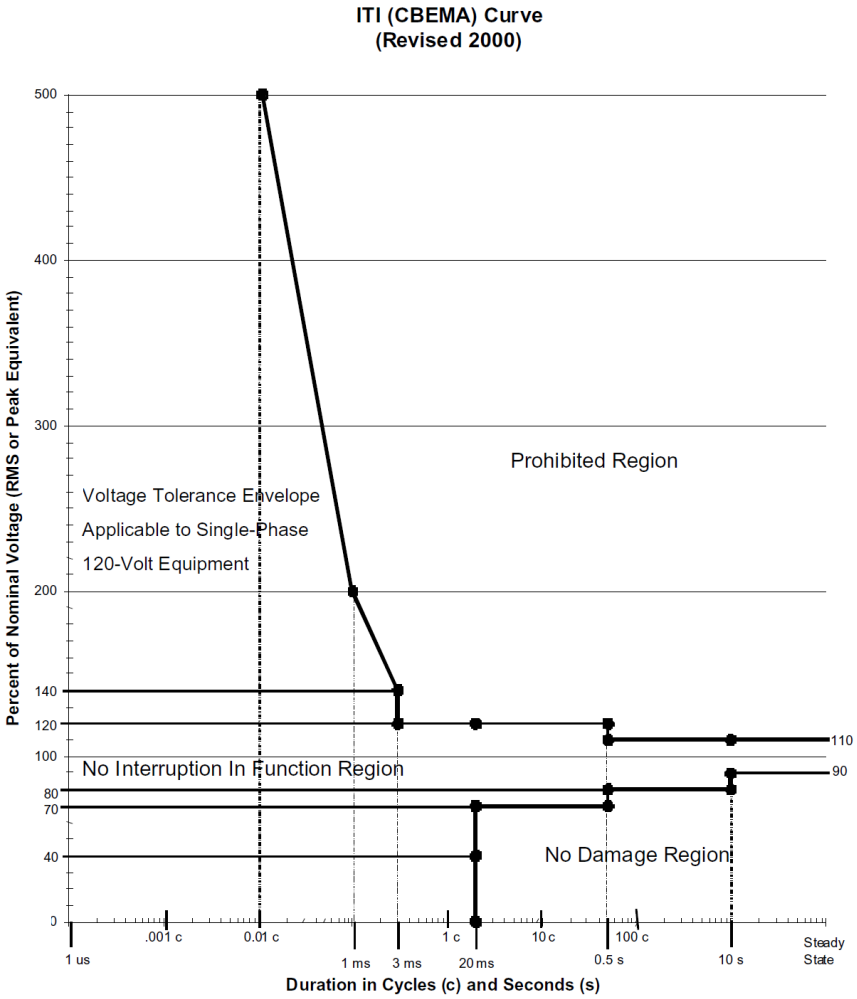

Figure 2.10: ITI/CBEMA acceptable voltage operation ranges. [32]

CHAPTER 3: DESCRIPTION OF THE PV SYSTEM

3.1. Components of the microgrid

3.1.1. PV source - solar panels

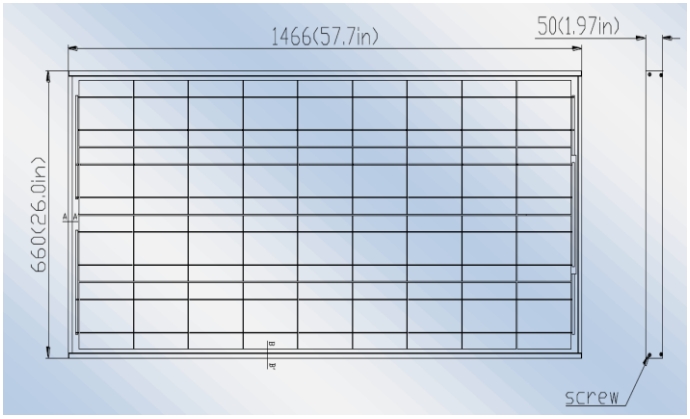

Figure 3.1: Solartech SPM130P-S-N (reference) front view. [33]

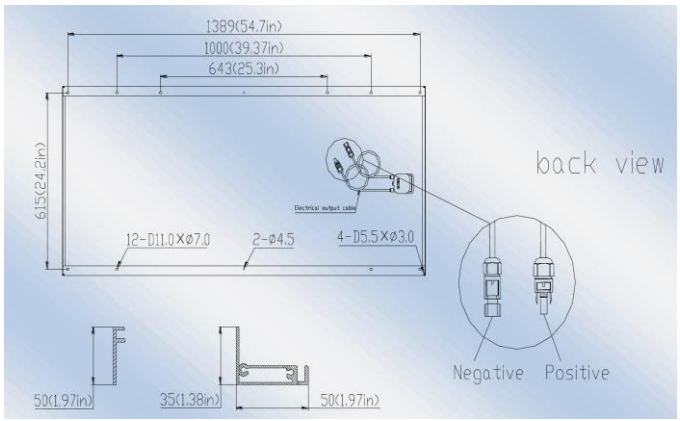

Figure 3.2: Solartech SPM130P-S-N (reference), back and side views. [33]

Table 3.1: Solartech SPM130P nameplate specifications

Rated maximum power	Pmax	130 W
Current at Pmax	Imp	7.35 A
Voltage at Pmax	Vmp	17.7 V
Short-Circuit Current	Isc	7.92 A
Open-Circuit Voltage	Voc	22.1 V
Nominal operating cell temperature	TNOCT	50 C
Maximum voltage	1000 V	
Cell technology	Poly-si	

*All technical data at standard test conditions: 25C (77F), 1 kW/m^2, AM 1.5.

3.1.2. Inverter

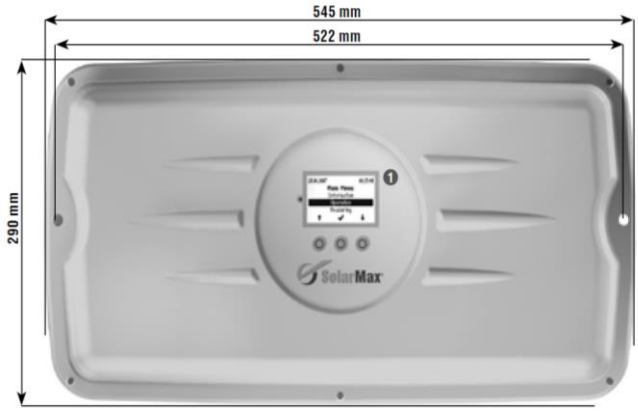

Figure 3.3: SolarMax 2000S inverter, front view. [34]

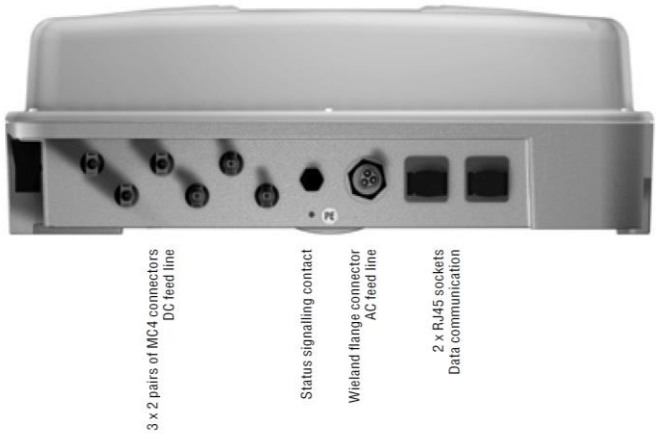

Figure 3.4: SolarMax 2000S inverter, bottom view. [34]

Connection

The Inverter includes an AC feed line connector (which comes from the main power grid and is connected to the loads), and three pairs of MC4 connectors for the DC lines. The on/off switch is in one of its sides. See layout in Figure 3.3 and 3.4.

The front display shows general information about the language, configuration, and values of current, voltage and power as shown in the datasheet. Next to it there is a LED that changes its color according to the conditions of operation of the system.

Components block diagram

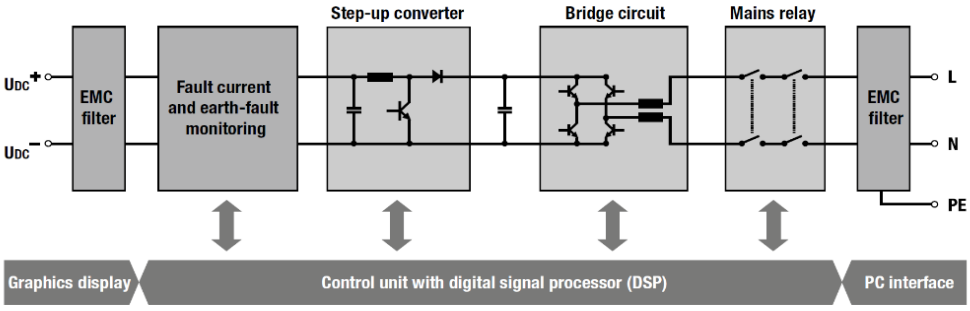

Figure 3.5: Block diagram of the inverter. [34]

The DC voltage of the solar generator is transferred to a DC bus voltage via a low-loss step-up converter. The IGBT bridge circuit generates the sinusoidal infeed current. The configuration parameters (password protected settings), as displayed in the menu, are the following:

Table 3.2: Configuration values of the inverter

Parameter	Value	Unit
Country	-	Other
Vac max	264	V
t Vac max 1	200	ms
Vac min	196	V
t Vac min 1	1500	ms
Vac 10 min max	253	V
Iac max	12	A
Pac max	1980	W
S max	1980	VA
Ierr max	300	mA
Iac mean max	1000	mA
f min 1	59.3	Hz
tf min 1	500	Hz
f max 1	60.5	Hz
tf max 1	500	ms

Conditions under which the system does not start/turns off: [34]

- When there is not enough DC current or voltage feeding the inverter. In such case, the device turns off without any previous notice.
- If the temperature sink within the inverter rises over 80° C. As a reference, ambient temperatures over 45° C would reach 75° C within the inverter and the output starts to decay.
- In the event of an earth fault, the system would detect the differential current and interrupt the mains operation. The safety mechanism included in the system would switch the device off.
- If there is no energy consumption: during the night or at times of insufficient irradiance the system eventually turns off after showing a warning on the display.

3.1.3. Loads

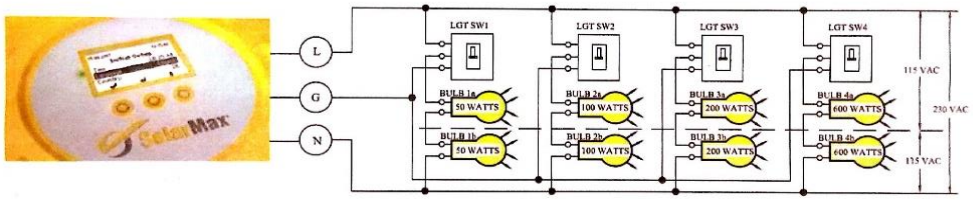

Figure 3.6: Detail of the connection of the loads. [35]

The loads' connection is relatively simple: 4 strings of light bulbs are connected in parallel, each one containing two of them in series and one respective switch. The four strings are connected to the same voltage, ground and neutral. We can notice in Figure 3.6 that the light bulbs have different rated power between each string. Then, if the voltage was not enough to feed the system, some of the strings (those at the very end) would just not light up when we require more energy than what the system provides.

3.1.4. Batteries

Figure 3.7: Battery type NP24 12B. [36]

Specifications

Model Genesis NP24 12B; type sealed lead acid, rechargeable; voltage 12 Volts; capacity 24 Ah; terminals bolt-type.

3.1.5. Data measurement devices

- Transducers: acuAMP DCT100-42-24-F

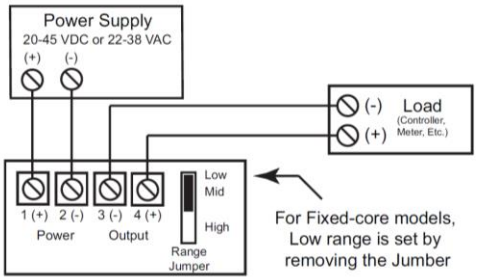

Figure 3.8: acuAMP DCT100-42-24-F connection diagram. [37]

Specifications

DC current transducer; fixed-core; power supply 20-45 VDC, 22-38 VAC; input ranges 0-50, 0-75, 0-100A (jumper selectable, see Fig. 3.6); output signal 4-20 mA sourcing, 24 VAC/DC; response time 20ms; output load 500 Max; output limit 23 mA.

- Current transformers: CR Magnetics CR2 RL

Figure 3.9: Current transformer, RL model. [38]

Specifications

Basic accuracy 10% FS or better (ANSI); thermal drift 100 PPM/°C; operating temperature -20° C to +75° C; installation category CAT II; pollution degree 2; insulation voltage 3500 VAC/1min; frequency range 50Hz - 400Hz; current ratio 100:5; accuracy AT 60Hz ± 1%; burden VA at 60 Hz 2.0.

3.1.6. Data acquisition relays

- National Instruments relay: NI-USB-X device

Our microgrid is using National Instruments USB X model 6163 OEM, custom made for DAQ. The National Instruments website indicates that the system pinout can be obtained from the Open Measurement & Automation Explorer (MAX) software by expanding the section “Devices and Interfaces” and right-clicking our device. [39] Despite the system we are using is indeed recognized as a USB-6363 by the provider’s software MAX, the pinout was not accessible this way. When tried to do so, the following message appears: “Unable to launch device pinouts. Confirm the

driver software is installed". To overcome this problem, the pinout was obtained from the respective manual as seen in Figure 3.10, and further verified by running experiments for signal recognition at each one of the relevant pins:

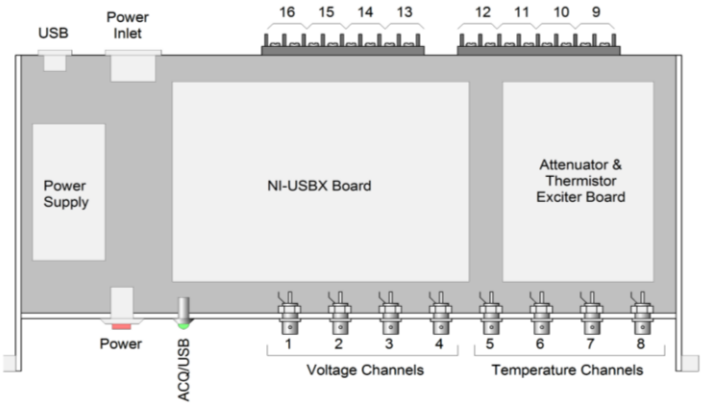

Figure 3.10: NI custom-made relay. [40]

The low signal ports only accept up to 10 V, whereas the rear of the NI device (pins 16 on) can handle as high as 600 VDC/VAC.

- Arbiter relay: Arbiter 1133A Device

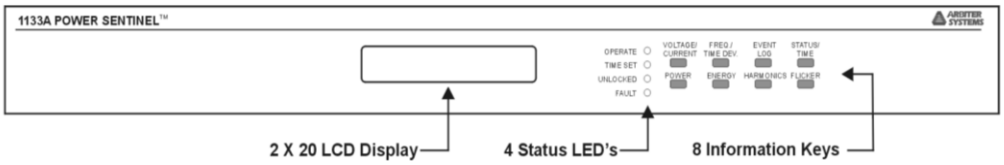

Figure 3.11: Arbiter 1133A relay, front view. [41]

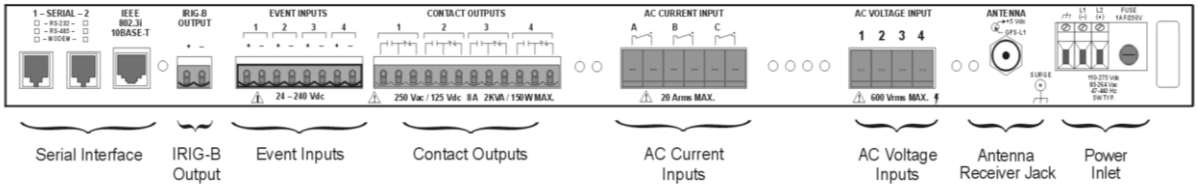

Figure 3.12: Arbiter 1133A relay, rear view. [41]

Table 3.3: Arbiter DAQ acceptable limits.

Maximum voltage	600 V RMS.
Maximum current	20 A RMS.

3.2. Wiring diagram of the system

3.2.1. Original projection

Figure 3.13 shows the layout of the original project when all its components are connected. The microgrid in the Power Systems Automation Laboratory, besides counting with a photovoltaic (PV) generation source, is also capable to integrate wind generation and battery storage. Storage is usually included in autonomous systems so that surplus generated energy is saved for moments when the load requires more energy than what can be produced. As a result, an autonomous microgrid can provide a continuous power supply within good quality standards.

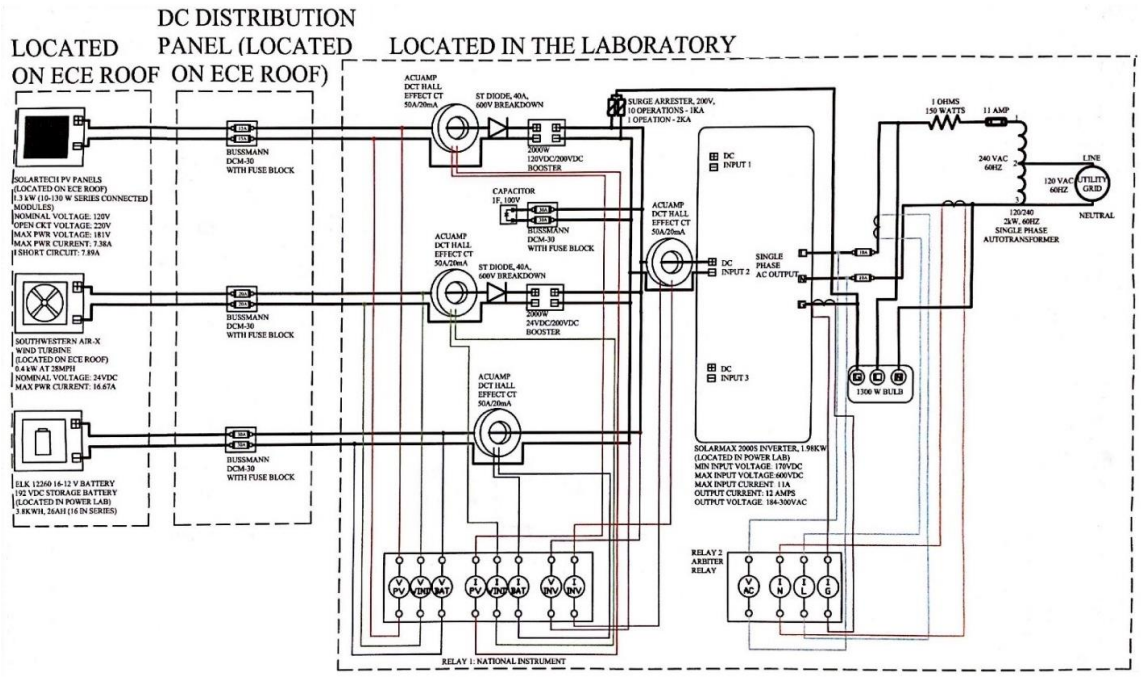

Figure 3.13: Diagram of the microgrid. [35]

3.2.2. Module at the beginning of this project

The last project in which this module was involved corresponds to the Ph.D. dissertation of Dr. Aniemi Umana in 2015 [35]. The microgrid had been used to test new strategies for protection of power systems and the analysis included simulations using the Win-IGS software. According to the diagram in Figure 3.14, The PV panels were the only source of energy, whereas the wind turbines were not connected. The battery bank was not connected to the system either.

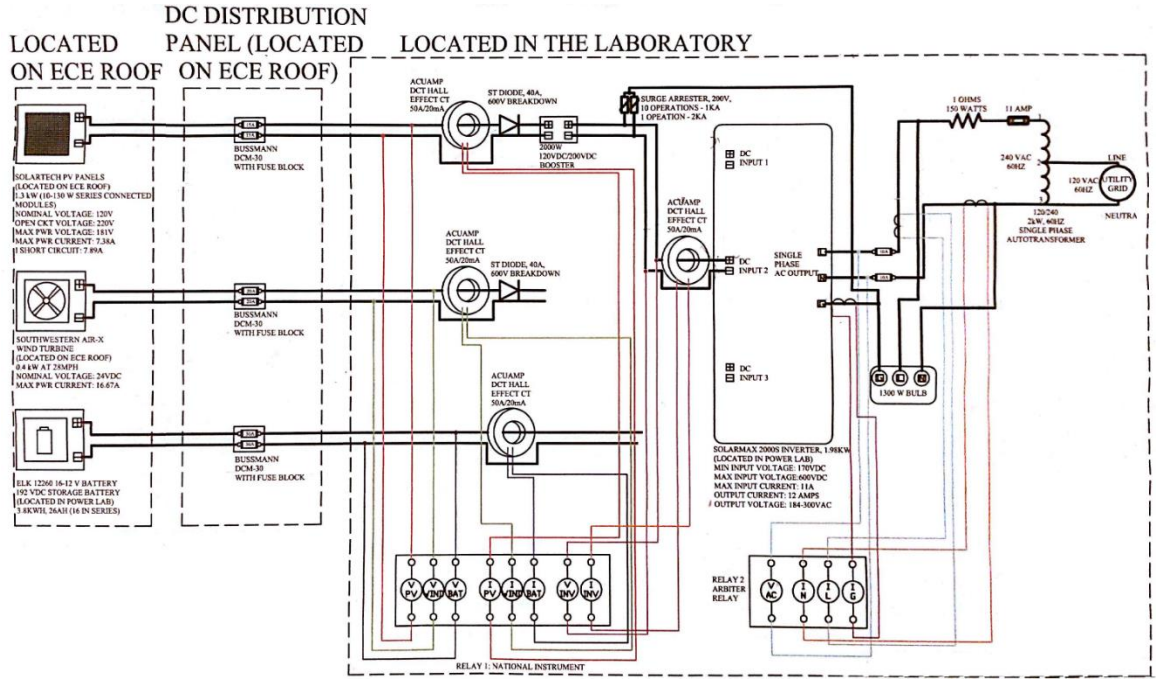

Figure 3.14: Diagram of the microgrid. [35]

For that project, the solar panels were the only power source in the microgrid that feeds the Inverter. The output of the inverter, 240 VAC (RMS), was connected to both ends of an autotransformer. On the other side, half of the windings of the autotransformer was connected to the bulk power grid to receive 120 VAC (RMS). The load of the system was connected to the 240 VAC zone.

Regarding measuring and DAQ devices in that project, the following characteristics can be noticed from Figure 3.14:

- There are four Hall-effect current transducers that were measured the PV and wind sources current, batteries net current, and the net current coming to the inverter. The output currents of these devices (5-20 mA) were read by the National Instruments Data Acquisition Device (DAQ).

- The National Instruments DAQ also took lectures from three DC different voltages, which came from the batteries, PV source, and wind source respectively.
- The system was set up to measure 3 different AC currents using current transformers (CTs): one from the hot wire (L), another from the neutral wire (N) and the last one for the ground (G). The Arbiter DAQ receives readings from these three currents, along with the voltage coming from both DC phases of the inverter.

3.2.3. Modifications and present set up of the PV Module

Originally, the module was found in the following conditions:

- Out of the four 5-20 mA current sensors, just one of them was connected and powered to take measurements from the PV module. The measurements went to the National Instruments Relay.
- None of the secondaries of the current transformers were connected. Neither were the AC voltages to be measured by the NI DAQ.
- The wires coming from the wind turbines and those from the batteries were not connected to the system either.
- The wires from the autotransformer were not set to be connected to the power grid.

After labeling all the wires of the circuit and making the connections necessary to power the photovoltaic system and to acquire data from its sensors, the result is the following. View Figures 3.15 and 3.16:

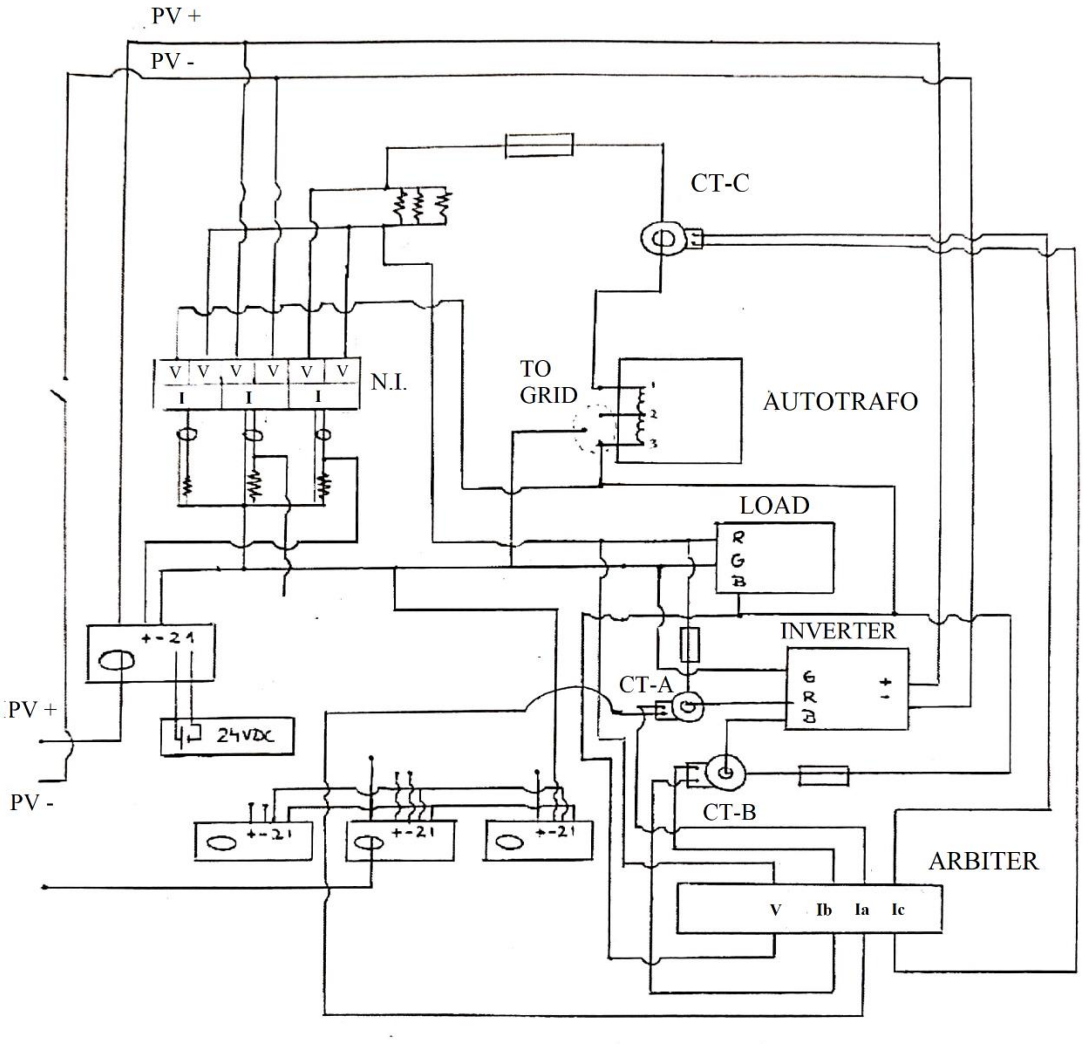

Figure 3.15: Diagram of the PV system connections in the present.

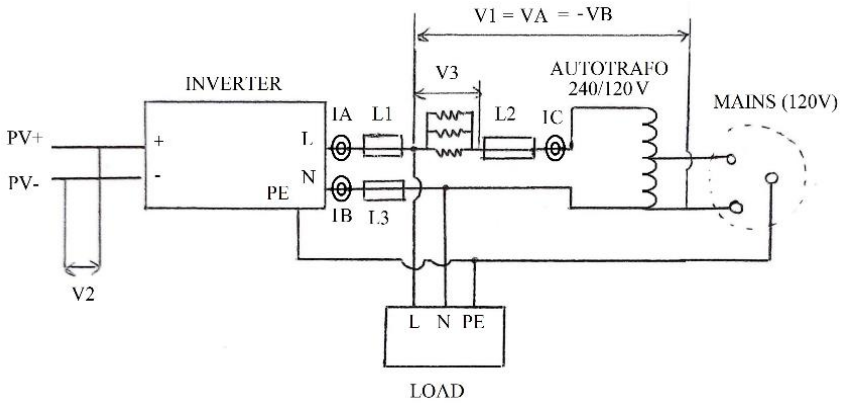

Figure 3.16: Simplified diagram of the microgrid system.

The changes with respect to previous conditions are:

- The autotransformer is now connected to the grid, which allows the interconnection of the 120/240 rated volt systems.
- The Arbiter Relay is reading the AC output voltage of the inverter, and three different currents: from the hot wire (L), the neutral (N) and the Ground (PE).
- The National Instruments relay is also reading three voltages: one DC voltage coming from the PV panels, one AC voltage coming from the autotransformer (proportional to the current flow in the mains grid) and the other one is the AC voltage feeding to the load.

3.3. Set up and configuration of the DAQ systems

3.3.1. Arbiter Systems device for phasor-based readings

Connection types

According to the Arbiter 1133A manual [41]**,** there are 6 types of connections that can be configured for our device to read values from. It is necessary to make sure the proper connection type has been chosen, as well as that the values to be read lay within the acceptable limits for both voltage and currents for the device or else the measurements recorded will not be valid.

Table 3.4: Arbiter data measuring configurations types. [41]

DSP notation	Explanation
1Ph2W1E	Single-Phase, Two-Wire, One-Element Circuits with Current and Potential Transformers
1Ph2W1.5E	1133A Single-Phase, Two-Wire, One and One-Half Element Circuits with Current and Potential Transformers
1Ph3W2E	1133A Single-Phase, Three-Wire, Two Element Circuits with Current and Potential Transformers
3Ph3W2E	Three-Phase, Three-Wire, Two-Element Delta Circuits with Current and Potential Transformers
3Ph4W2.5E	Three-Phase, Four-Wire, Two and One Half-Element Circuits with Current and Potential Transformers
3Ph4W3E	Three-Phase, Four-Wire, Three-Element Circuits with Current and Potential Transformers

Our system is set up to take measurements from three different zones. They would be current from line 1 (CT-A), return line or neutral (CT-B), which both come from the inverter, and line 2 which is coming from the grid (CT-C).

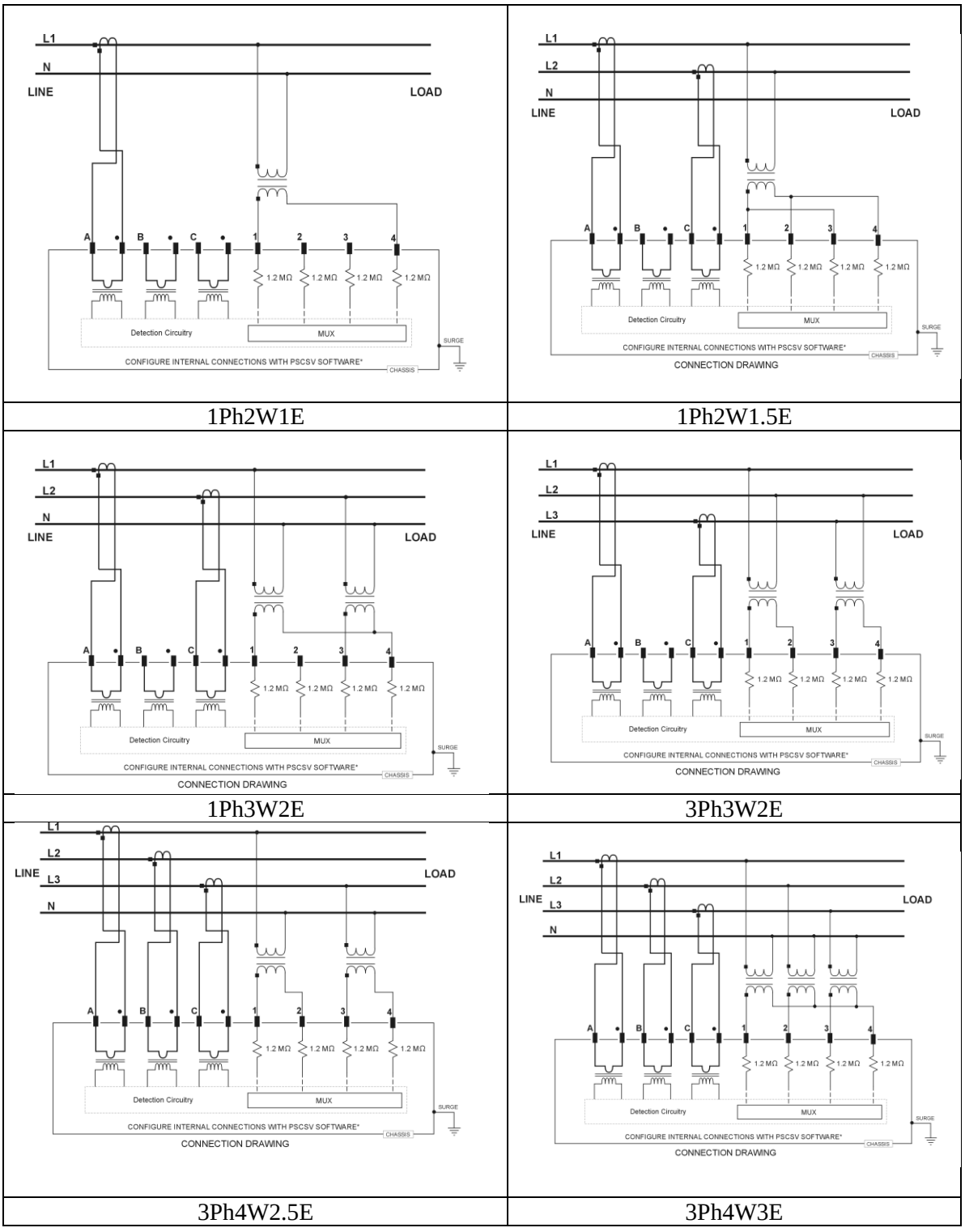

Figure 3.17: Arbiter connections types to measure data. [41]

Table 3.5: Fitness of Arbiter configurations for this project.

Connection	Does it fit the PV system?	Reason
1Ph2W1E	No	One line is missing
1Ph2W1.5E	No	Voltage measurement between line 1 and line 2 is necessary, since $V_{L1} \neq V_{L2}$.
1Ph3W2E	No	Voltage measurement between line 2 and neutral is necessary, since $V_{L2} \neq V_N$
3Ph3W2E	No	Voltage measurement between line 1 and line 2 is necessary, since $V_{L1} \neq V_{L2}$
3Ph4W2.5E	Yes	Since there is no voltage measurement between line 3 and N, $V_{L3}=V_N$ which holds for this project.
3Ph4W3E	No	Voltage measurement between line 2 and neutral is necessary, since $V_{L1} \neq V_{L2}$

Settings using Power Sentinel SCV:

The Arbiter's software is called Power Sentinel CSV, which can be downloaded from the manufacturer's website. After physically connecting the user's laptop to the device, it is necessary to establish a connection. This can be done using the toolbar, clicking on "Connection", then clicking on "Open" and following the additional steps corresponding to the specific physical connection from the manual.

For this thesis, after establishing a TCP connection (see parameters in Figure 3.18), use the "Log in as" command and choose the right parameters for user and password. This will enable other additional features to change the configuration parameters of the system. The right connection and settings were chosen in the window that appears after clicking on "Measurement Parameters". See figure 3.19.

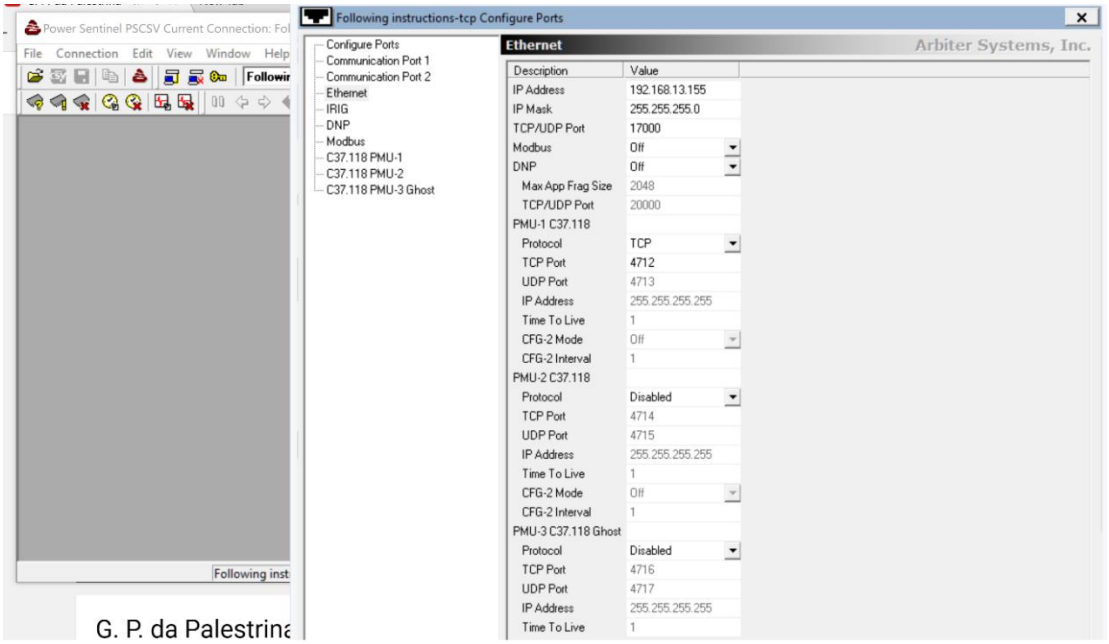

Figure 3.18: Arbiter System ports configuration.

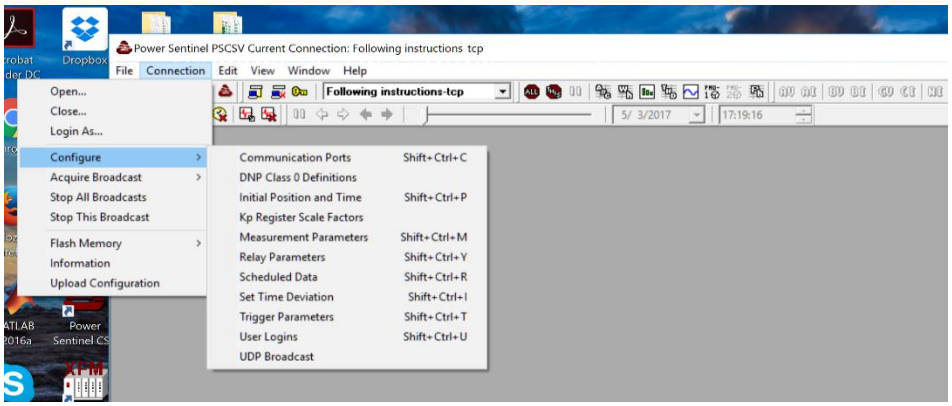

Figure 3.19: Arbiter System parameters settings.

Settings using the WinXfm software:

The Arbiter device has the capability to record phasor-based data using the software WinXfm. To do so, we are required to obtain the right parameters from the Arbiter system through the command “Connection”, “Ethernet”.

The parameters necessary to establish a connection of this type are I.P. address, TCP port, login, and password, and PMU-1 TCP port number.

The second step is to enter to the software WinXfm and press the button “PMU Client” from the toolbar. Then, we introduce the parameters attached to the back of the device. See Figure 3.20.

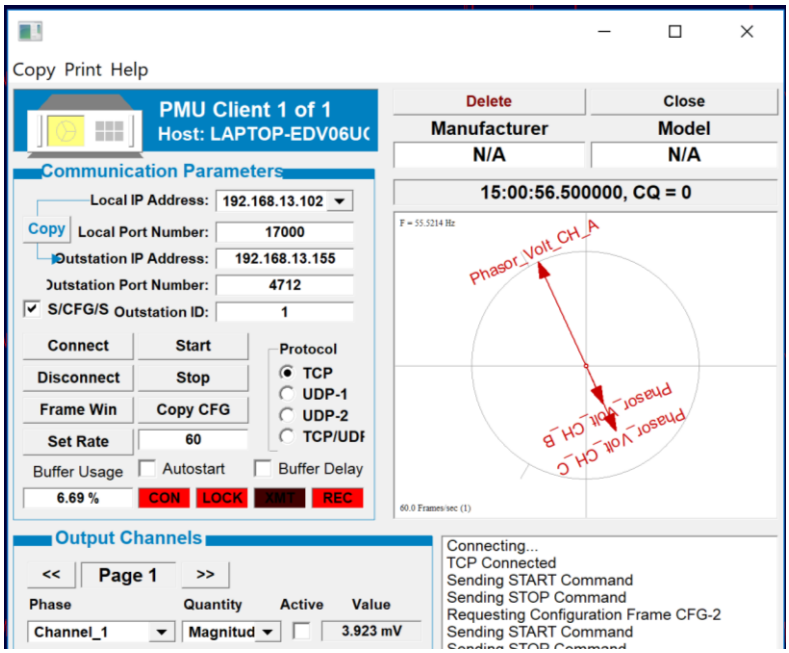

Figure 3.20: Arbiter System measurements settings

The third step is to activate the output channels we are going to use by marking their boxes that are at the bottom of the windows as seen in Figure 3.20. For each phasor, the system allows us to display any of the following options: magnitude, angle, frequency, dF/dt, real, and imaginary components. The equivalence between the channels that appear in that window can be seen in Table 3.6:

Table 3.6: Arbiter System measurement parameters

Channels	Channel 1	Channel 2	Channel 3	Channel 4	Channel 5	Channel 6
Phasors	Voltage A	Current A	Voltage C	Current C	Voltage B	Current B

These channels are only available to be seen and recorded once a connection has been established and the data acquisition has started. That is, by selecting “connect” and “start” in that window. That same window is the one that controls the data acquisition and not the WinXfm toolbar anymore.

To see the channels, it is necessary to press “select channels to display” in the main toolbar and add each one of the channels to the list of displayed channels. In addition, there is a delay between the moment we decide to stop the acquisition and the moment it is fully stopped, which is related to the buffer capacity and the time required for the communication to be completed.

3.3.2. National Instruments device for waveform-based readings

Connection and settings

Figure 3.21: Front side of the NI USBX

Table 3.7: NI USBX Device channels allocation, front side

		Channels								Type
Front panel	WinXFM channel (ai)	16	17	18	19	20	21	22	23	(+)
		24	25	26	27	28	29	30	31	(-)
	Physical name	1	2	3	4	5	6	7	8	Differential
		Voltage				Voltage				

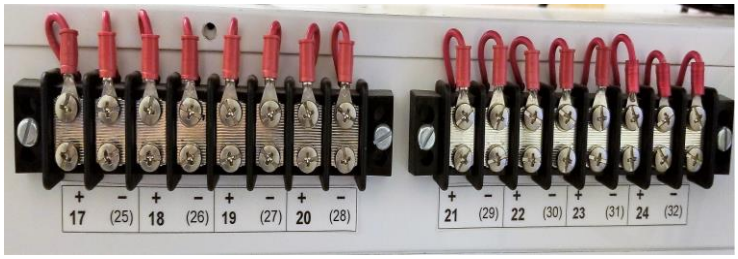

Figure 3.22: Rear side of the NI USBX

Table 3.8: NI USBX Device channels allocation, rear side

		Channels								Type
Rear panel	Physical name	17	18	19	20	21	22	23	24	(+)
	WinXFM channel (ai)	0	1	2	3	4	5	6	7	
		8	9	10	11	12	13	14	15	(-)
	Physical name	25	26	27	28	29	30	31	32	
		Voltage								

For our case, what we have is the following: The National Instruments relay is connected to a 120 VAC (RMS) supply which comes from the bulk power grid. Our signals are differentially computed by the WinXfm Software, which takes the relevant signals as a subtraction of two channel's measurements. These measurements will be discussed in chapter 4. See Figure 3.19 and Table 3.7 for the front side configuration, and Figure 3.20, and Table 3.8 for the rear side configuration of the NI DAQ device.

3.4. Sensors and DAQ calibrations

3.4.1. Current transformers: used in this project to measure AC currents

The original ratio of the current transformers used and described previously is 100:5 A, where the first digit corresponds to the total magnitude to be measured (the primary side) and the second to the output signal (the secondary side). For this project, the connection was made wrapping four loops in the primary. Therefore, the new ratio is 25A in the primary to 5A in the secondary, which is equivalent to a turns ratio of 5:1. After checking the values for each one of the current transformers by the use of multimeters, clamp meters, and an oscilloscope, it was noticed that not all the CT followed the 5:1 ratio, and the error varies according to the connection and load (resistance) that is faced by the transformer.

An experiment was realized to set the calibration parameters that reflect the best the ratio of the current transformer. Additional information can be found in the appendix. This set up of the CTs does not connect to varying loads from the NI DAQ device or other resistances to reduce inconsistencies in the CT transformation radios, which were found in other types of connections.

Table 3.9: AC current transformers parameters

Current Transformer	Isec: Iprim.	I primary
1 (CT-A)	5.2/1	InvAC “L” Line
2 (CT-B)	5.2/1	InvAC “N” Line
3 (CT-C)	5/1	Grid “XFMR”+ Line

3.4.2. Current sensors: used in this project to measure DC currents

The input of the current sensors varies in three different scales (0-50, 0-75 and 0-100 A). The output is a signal for 4-20mA. For this case, we have used the first range to get a more accurate scale. The relationship is found by linear interpolation based on Thales' intercept theorem. See Table 3.10. Since all the channels of the NI DAQ device measure voltage and not current, the module counts with resistors that can be used to calculate the current flowing through them. Some correction factors have been added to such resistances and values for each sensor so that the measurements keep consistency and precision among them.

Table 3.10: DC current transducers parameters

Current Sensor	Equation y=f(x) Isec (A) vs Iprim (A)	Equation x=f(x) Iprim vs Isec (A)	Iprim	Isec= Vmeasured/R
1 (PV+)	$y=(4.121+0.32x)*10^{-3}$	x=3125y-12.878	"PV+" Line	VDC/50.35
3 (Inv DC)	$y=(4.472+0.32x)*10^{-3}$	x=3125y-13.975	InvAC "B" Line	VinvDC/50.35

Note: The third current sensor was calibrated and used in a previous connection scheme but won't be used for the experiments included in this project.

3.4.3. Voltage readings from the NI device

The calibration weights for the National Instruments device are for instant values, and not for RMS values. See Table 3.11. On the other hand, the Arbiter system can record values as RMS. The parameters were found after experiments to determine which of the ports correspond to a particular reading.

Table 3.11: Voltage calibration parameters

Signal	Weight	Measurement	Units
a0-a8	x100	Rear_1_Grid	V
a1-a9	x100	Rear_2_PV	V
a2-a10	x100	Rear_3_load	V
a16-24	x1	V_inv_AC	V
a17-a25	x1	V_alpha_grid	V
a18-a26	x1	V_pvDC	V

3.5. Connected operation: limits

- PV DC voltage: according to the specifications of the system, there are 10 panels in series. Therefore, we use 10 times the Voc as a first approximation to the maximum voltage. That is 10x22.1=221 V. The voltage, however, will be closer to the maximum power point voltage (Vmpp), which is 17.7 under nominal atmospheric conditions.
- PV AC current: since the 10 solar panels are connected in series, they keep the current of a single panel. As a first approximation, the limit would be the short-circuit current: Isc=7.92 Ac. The actual current would be closer to that at the maximum power point, which is 7.35A under nominal atmospheric conditions.
- Load: the current depends on how many light bulbs are switched on. The voltage is nominally 240 V AC but depends on the main grid. If we consider the light bulbs as purely resistive, for referential purposes, the maximum current value is 5.05 A AC, for all light bulbs on. See Table 3.12, and the connection diagram previously depicted in Figure 3.4.

Table 3.12: Current consumed by the load, per light bulbs row.

	Rated values			Current at 120 V
Row	P (W)	V (V)	R=V^2/P (Ω)	I=V/R (A)
1	50	120	288	0.42
2	100	120	144	0.83
3	200	120	72	1.67
4	300	130	56.33	2.13
			Total Max.	5.05

- Inverter, load, and grid currents:

From Figure 3.14, the simplified diagram of the inverter, we can apply Kirchhoff's current law to get

$$IG = IL - IM \qquad (6)$$

where *IG* is current from the Bulk Grid, *IL* is current to the load, and *IM* is the current from the microgrid, which is the same as the inverter output current. This relationship takes the sign convention that both bulk grid and microgrid are generating, so it is positive for current coming from them, and can only receive current, so it is positive for current coming into the load.

It must be noticed that those three currents are AC, and not necessarily in phase. If we consider all cases possible for current and shift angle, the expected limit for a maximum current going into or coming from the grid is 12.97 AC. See Table 3.13.

Table 3.13: Maximum AC RMS values during normal operation.

I load (A)	I inv (A)	I grid (A) = I load - I inv
0	0	0
0	7.92	-7.92
0	-7.92	7.92
5.05	0	5.05
5.05	7.92	-2.87
5.05	-7.92	12.97
-5.05	0	-5.05
-5.05	7.92	-12.97
-5.05	-7.92	2.87

CHAPTER 4: DISCUSSION OF RESULTS

4.1. Configuration of DAQ systems

For the experiments run in this project, the following settings have been used:

4.1.1. NI system: measurements as waveforms, using software WinXfm

Table 4.1: WinXfm settings used to read from NI DAQ.

Signal	Weight	Name	Units	Data obtained	Scale signal to data	Units
a0-a8	x100	Rear_1_Grid	V(t)	Inverter output AC voltage	x1	V(t)
a1-a9	x100	Rear_2_PV	V(t)	Solar panels DC voltage	x1	V(t)
a2-a10	x100	Rear_3_load	V(t)	Voltage proportional to the current from main grid	x1	V(t)
a18-a26	x1	VR_pvDC	V(t)	PV DC current	(VR_pvDC/50.35) x3125-12.878	A(t)

4.1.2. Arbiter system: measurement as phasors using Power Sentinel CSV software.

Table 4.2: PSCSV settings used to read from Arbiter DAQ.

Signal	Weight	Measurement	Units	Data obtained	Notes
I A’	x1	Current A’ (L1)	A rms	Inverter output AC current	Phase A
I B’	x1	Current B’ (L3 = N)	A rms	Return line AC current	Neutral
I C’	x1	Current C’ (L2)	A rms	Transformer secondary AC current	Imains=2*Isec_trafo
V A’	x1	Voltage A’ (L1-N’)	V rms	Inverter output AC voltage, phase A	Phase A – neutral (B), same as V load
V B’	x1	Voltage B’ (L2-N’)	V rms	Transformer secondary AC voltage	Vmains=1/2*Vsec_trafo
V C’	x1	Voltage C’ (L3-N’)	V rms	None	Necessary to define L3=N

L1=A’=PhaseA L2=B’=Grid L3=C’=Return=B=External neuter N=Internal neuter

4.2. Characterization of the energy supply

4.2.1. Harmonic analysis

4.2.1.1. Settings

- Procedure for the Arbiter system:

The Arbiter 7.8.2 PMU Setup Terms and Definitions Manual [41] includes the following information with respect to the program settings:

- Open the PMU-1 and PMU-2 setup window by selecting Connection > Configure > Communication Ports, or by clicking the Configure Ports button and selecting PMU-1 or PMU-2.
- Window Length sets the integer number of measurements averaged for stability; small values give faster readings; values range from 1 to 24, do not set to zero.
- Estimated Rate, rate values are different for 50 Hz (1, 2, 5, 10, 25, 50) and 60 Hz (1, 2, 3, 4, 5, 6, 10, 12, 15, 20, 30, 60).

- Limitations of both systems:

- The Arbiter system does not show results over the 13^{th}-order harmonic.
- The Arbiter system only records THD every 1 second, and the computations are done internally. Even when logged in as admin, it is not possible to access the internal computations but only their final results.
- The National Instruments relay can't record and transmit data sampled at 8kHz for a window of 600 seconds. Therefore, the system is only considering very short harmonics (3 seconds), with samples recorded for up to 10 seconds.

Signals that were taken into consideration

Table 4.3: Measured signals relevant to this project. See Table 4.1.

Type	Data obtained	Measurement	DAQ
Waveform and phasor measured	V out Inverter =Vload	Rear_1_Grid	NIX, ARB
Waveform to be calculated, phasor measured	V sec transformer=2 Vgrid	Rear_1_Grid,-Rear_3_load, V B' (phasor)	NIX, ARB
Phasor measured	I out inverter	I_inv_AC, I A'	NIX, ARB
Phasor measured	I sec transformer=1/2 IGrid	I_alpha_grid, I C'	NIX, ARB
Phasor to be calculated	I load	I_inv_AC- I_alpha_grid, I A' – I C'	NIX, ARB

The approach to follow is to do a harmonic analysis through the waveform measurements and use the phasors-based measurements to check the calculations from the waveforms. The reason behind it is that the Arbiter system does not allow us to obtain all the measurements at a high frequency, which is necessary to calculate harmonics indexes. Instead, it gives us the results of a harmonic analysis for every 1 sec.

Codes implemented

The full program written for the harmonic analysis can be found in the Appendix, while a pseudocode of the program is in this section. A version of the program "read_comtradefull" obtained through MATLAB exchange website was implemented and modified to fit the purpose of this project.

- Harmonic Analysis:

Clear display and variables

Use function read_comtradefull to read the data from NI Arbiter device

Set parameters: sampling period, length of signal, discrete time vector

For all three-seconds sets

Take only a three-second set

For each of the 12-cycle windows in that part

Apply fast Fourier transform (FFT) to one window

Consider only half (a single side) of the frequency spectrum

Apply factors to keep the equivalent energy of waveform the same

(Optional: reconstruct signal)

For all 50 harmonics

Group central harmonics and their +- 5Hz bins

End

Save harmonics in an array

End

Calculate each order harmonic

Calculate total harmonic distortion

End

Show results

- Signal reconstruction 1: (Optional)

Set a time vector

Set zero frequency component of the FFT as offset of reconstructed waveform

For all frequencies different from zero

Compute sin(2*pi*f*t+phase)

Find the phase angle that fits the original waveform the best

Add sin(2*pi*f*t+ corresponding phase) to reconstruction accumulator

End

Plot original vs. reconstructed signals

- Signal reconstruction 2: (Optional)

Apply techniques for inverse fast Fourier transform

Initial verification of results:

To show the coherence of the measurements and computations, the outputs of the code for harmonic analysis have been compared to those indexes calculated internally by the Arbiter Relay.

4.2.1.2. Initial tests

Date: 09.20th.17, 22:53:00 UTC (6.53 pm). Measurement: inverter AC output voltage.

- Fast Fourier transformed signal:

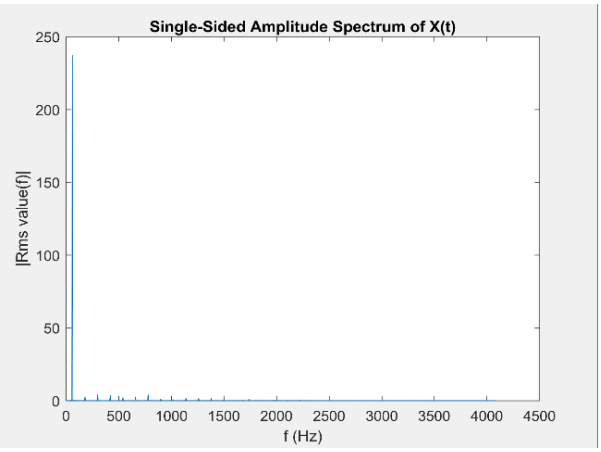

Figure 4.1: Amplitude spectrum for inverter V AC.

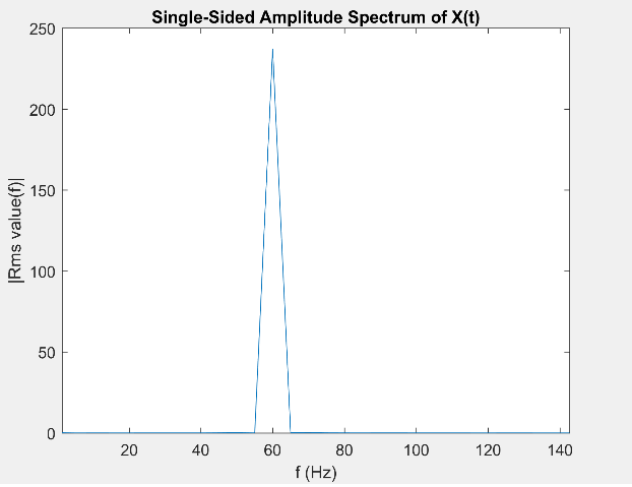

Figure 4.2: Zoom-in of amplitude spectrum for inverter V AC.

Both figures 4.1 and 4.2 correspond to the Fourier Transform of the same signal. When zoomed in, the peak amplitude is noticeable for 60 Hz, corresponding to the standard mains frequency, and so are the bars for other harmonics components with much lesser amplitude.

- Signal reconstruction:

Figures 4.3 and 4.4 correspond to 12-cycle windows of the inverter AC voltage ("Rear_1_Grid") sampled in different moments. Fig. 4.3 is at the beginning, and 4.4 at the middle of a 3 seconds period. Original (in blue) and reconstructed signal (in red) have been plotted in the same figure.

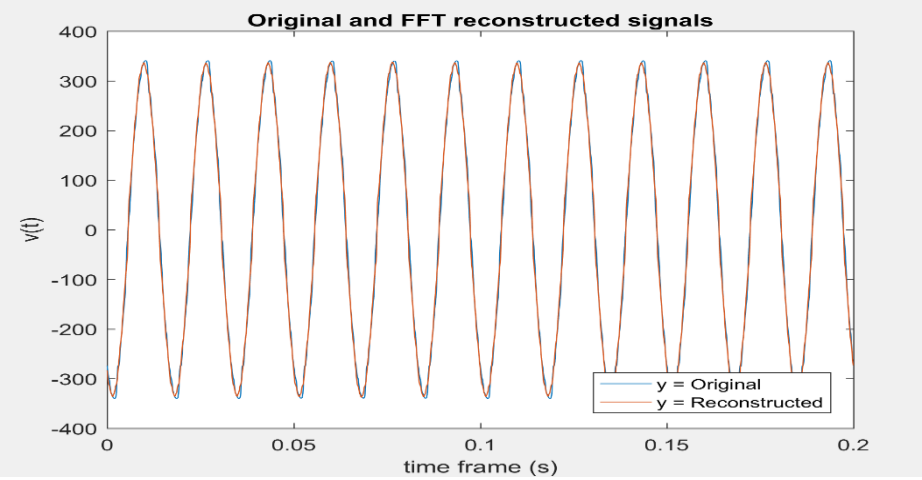

Figure 4.3: Original and FFT reconstructed signal for Inverter V AC.

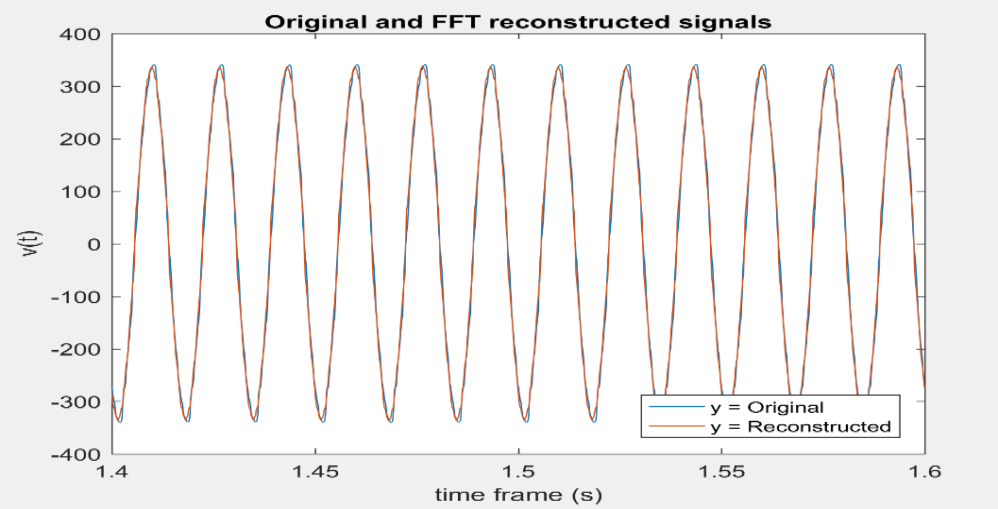

Figure 4.4: Original and FFT reconstructed signal for Inverter V AC.

- Accuracy of the system

Voltage: AC inverter voltage

Date: 9/20/2017, Approx. 6.53 PM. PV module ON, Load OFF

The limits for the magnitude measured each harmonic component using the Arbiter Systems device and the Power Sentinel CSV software have been surrounded in the graphic from Figure 4.5. Likewise, the results computed using the NI device and the code developed for this project have been underlined and can be noticed in Figure 4.6. Notice the readings up to the 12^{th} order harmonics are consistent among both methods.

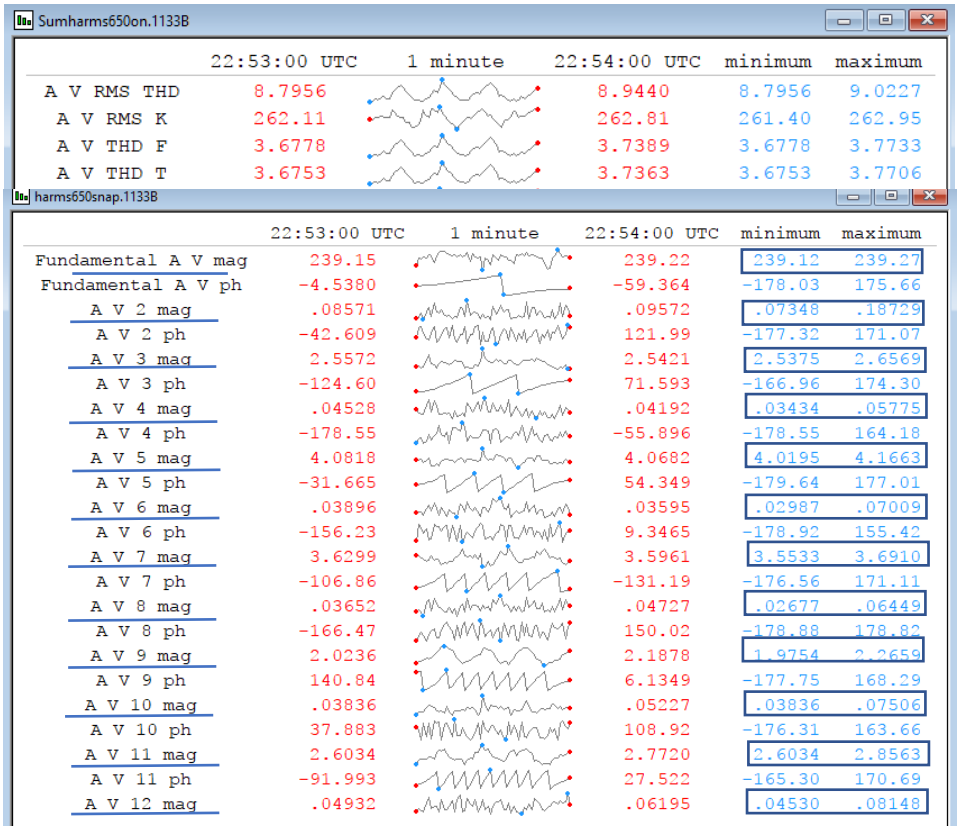

Figure 4.5: Arbiter Systems inverter VAC measurements

```
Fvs =

  Columns 1 through 15

  237.0261    0.1295    2.6280    0.0415    4.0219    0.0440    3.5648    0.0463    2.1692    0.0478    2.7029    0.(

  Columns 16 through 30

    0.0413    0.6113    0.0458    1.7915    0.0591    1.5239    0.0552    1.9085    0.0580    0.4876    0.1225    0.:

  Columns 31 through 45

    0.3035    0.0335    0.4235    0.0460    0.1831    0.0392    0.3148    0.0199    0.1035    0.0279    0.0280    0.(

  Columns 46 through 50

    0.0131    0.0396    0.0244    0.0660    0.0204


THDvTotal =

    8.8413    8.8645    8.9051


THDv_100 =

    3.7311    3.7394    3.7570
```

Figure 4.6: MATLAB-computed inverter VAC harmonics using NI DAQ.

The columns of Fvs are the individual harmonics value (RMS) calculated for every harmonic between 1 and 50, as a total value (not in %), in the same units as the results from the Arbiter. Notice all the harmonic values are within the limits recorded by the Arbiter system every second between 22:52:00 and 22:53:00. The values in percent scale are used for the indexes computation. See table 4.4.

Table 4.4: Harmonics recorded by Arbiter and NI devices.

	Date	09.20.17	6.53 pm	Direct	Voltage Load
	Min	Max	Measured	Min error	Min error (%)
1	239.120	239.270	237.026	0.009	0.876
2	0.073	0.187	0.130	0.000	0.000
3	2.538	2.657	2.628	0.000	0.000
4	0.034	0.058	0.042	0.000	0.000
5	4.020	4.166	4.022	0.000	0.000
6	0.030	0.070	0.044	0.000	0.000
7	3.553	3.691	3.565	0.000	0.000
8	0.027	0.064	0.046	0.000	0.000
9	1.975	2.266	2.169	0.000	0.000
				Total	0.88

Experiment date: 10/17/17, Approx. 3.54 PM. PV module ON, Load ON

Following the same procedure as in the previous experiment, the results in Figure 4.7, Figure 4.8 and Figure 4.9 are obtained.

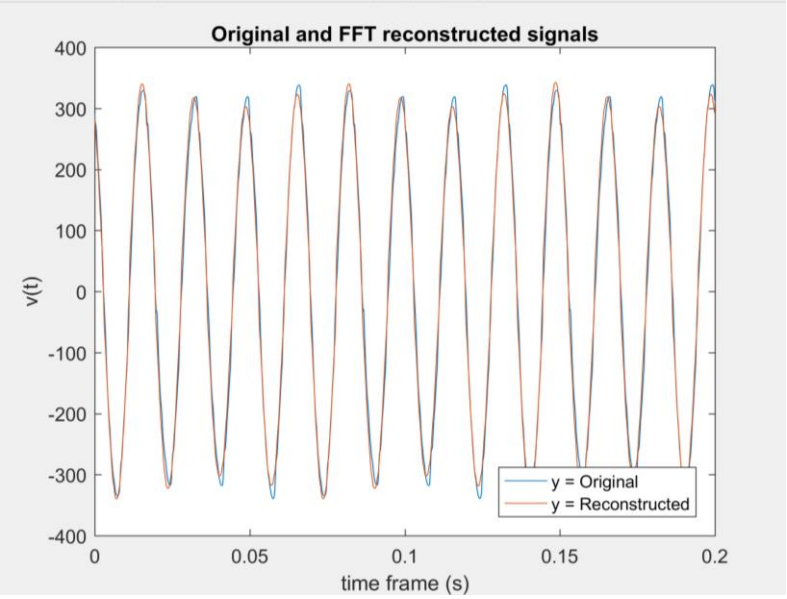

Figure 4.7: Original and FFT reconstructed signal for inverter VAC.

	15:54:50 PC	1 minute	15:55:50 PC	minimum	maximum
Fundamental A V mag	232.14		231.89	231.85	232.17
Fundamental A V ph	-176.63		66.819	-179.77	179.50
A V 2 mag	1.4574		1.4587	1.4304	1.4854
A V 2 ph	-51.296		124.52	-179.38	174.44
A V 3 mag	3.0611		3.1939	3.0611	3.1939
A V 3 ph	65.209		78.224	-171.88	178.81
A V 4 mag	.55050		.57600	.53817	.58293
A V 4 ph	7.9677		-167.87	-178.57	165.83
A V 5 mag	3.3751		3.4829	3.3151	3.4829
A V 5 ph	172.29		-50.644	-173.08	172.33
A V 6 mag	.46880		.46811	.44452	.48293
A V 6 ph	-66.576		-55.047	-171.12	166.75
A V 7 mag	3.0928		3.0225	3.0225	3.1343
A V 7 ph	135.21		39.262	-170.71	177.63
A V 8 mag	.25544		.26019	.24061	.27043
A V 8 ph	142.54		14.040	-178.55	179.76
A V 9 mag	2.0464		2.0994	2.0391	2.1042

Figure 4.8: Arbiter Systems inverter VAC measurements.

```
Fvs_100 =

  Columns 1 through 13

  100.0000    0.1404    1.3575    0.0489    1.3987    0.0729    1.2900    0.0287    0.8919    0.027
  100.0000    0.1290    1.3774    0.0584    1.3927    0.0716    1.2878    0.0331    0.9039    0.022
  100.0000    0.1325    1.3781    0.0625    1.3820    0.0627    1.2937    0.0318    0.8931    0.027

  Columns 14 through 26

    0.0218    0.4277    0.0446    0.2330    0.0272    0.6771    0.0239    0.4370    0.0241    0.438
    0.0167    0.4299    0.0445    0.2303    0.0298    0.6825    0.0232    0.4445    0.0265    0.444
    0.0205    0.4358    0.0470    0.2289    0.0379    0.6834    0.0438    0.4368    0.0306    0.458

  Columns 27 through 39

    0.1273    0.1393    0.1972    0.0489    0.0256    0.0377    0.0394    0.0179    0.0401    0.022
    0.1286    0.1359    0.2017    0.0548    0.0219    0.0369    0.0415    0.0151    0.0367    0.022
    0.1332    0.1357    0.1986    0.0532    0.0177    0.0381    0.0477    0.0144    0.0381    0.023

  Columns 40 through 50

    0.0202    0.0249    0.0107    0.0132    0.0096    0.0237    0.0067    0.0303    0.0099    0.012
    0.0223    0.0273    0.0084    0.0134    0.0119    0.0226    0.0069    0.0315    0.0110    0.014
    0.0202    0.0291    0.0075    0.0130    0.0120    0.0215    0.0075    0.0291    0.0107    0.013
```

Figure 4.9: MATLAB-computed inverter VAC harmonics using NI DAQ.

Table 4.5: Harmonics recorded by Arbiter and NI devices.

	Date	10.17.17	3.53 pm	Direct	Voltage Load
	Min	Max	Measured	Min error	Min error (%)
1	231.850	232.170	229.068	0.012	1.200
2	1.430	1.485	0.304	0.788	78.778
3	3.061	3.194	3.157	0.000	0.000
4	0.538	0.583	0.143	0.734	73.381
5	3.315	3.483	3.166	0.045	4.509
6	0.445	0.483	0.144	0.677	67.673
7	3.023	3.134	2.964	0.020	1.952
8	0.241	0.270	0.073	0.698	69.768
9	2.039	2.104	2.046	0.000	0.000
				Total	297.26

By checking the results of this experiment, we can notice that only even-order harmonics are much different in both devices. See Table 4.5. That suggests filtering or distortion of other kind that affects these devices differently, since the connections in both cases are direct from the points of measurement. To avoid great sources of error, even-order harmonics will not be considered in the analysis.

4.2.1.3. Results and discussion

List of events recorded

- NI device, voltages as waveforms

Table 4.6: Records of V waveforms using the NI DAQ

Date	Time	Time of the day	Sky condition	Full load	PV source
09.20.17	3.21 pm	Afternoon	Clear	OFF	OFF
	6.53 pm	Evening	Clear	OFF	ON
	6.58 pm	Evening	Clear	OFF	ON
10.17.17	11.20 am	Morning	Overcast	OFF	ON
	11.29 am	Morning	Overcast	OFF	ON
	11.42 am	Morning	Overcast	ON	ON
	11.45 am	Morning	Overcast	ON	ON
	3.21 pm	Afternoon	Scattered clouds	OFF	OFF
	3.43 pm	Afternoon	Scattered clouds	OFF	ON
	3.51 pm	Afternoon	Scattered clouds	ON	ON
	3.55 pm	Afternoon	Scattered clouds	ON	ON

- Arbiter, AC currents as waveforms, Arbiter on WinXfm:

Table 4.7: Records of V and I waveforms using the Arbiter DAQ

Date	Time	Time of the day	Sky condition	Full load	PV source
11.14.17	3.53 pm	Afternoon	Clear	OFF	OFF
	4.21 pm	Afternoon	Clear	ON	OFF
	4.31 pm	Afternoon	Clear	ON	OFF
	4.57 pm	Afternoon	Clear	ON	OFF

- AC Currents and voltages as phasors, Arbiter on PSCVS:

Table 4.8: Records of V and I phasors using the Arbiter DAQ.

Date	Time	Time of the day	Sky condition	Full load	PV source	Fluorescent lights
11.14.17	4.30 to 4.45 pm	Afternoon	Clear	ON	OFF	ON
	4.51 to 4.55 pm	Afternoon	Clear	ON	OFF	ON
	4.59 to 5.06 pm	Afternoon	Clear	ON	OFF	ON
11.20.17	10.53 to 11.30 am	Morning	Clear	OFF	ON	ON
	11.30 to 11.34 am	Morning	Clear	OFF	ON	ON
	11.40 to 11.53 am	Morning	Clear	ON	ON	ON

Table 4.8 (continued): Records of V and I phasors using the Arbiter DAQ

Date	Time	Time of the day	Sky condition	Full load	PV source	Fluorescent lights
12.07.17	16.42 to 16.50 pm	Evening	Overcast	OFF	ON	ON
12.23.17	17.58 to 18.13 pm	Evening	Overcast	OFF	OFF	ON
	18.18 to 18.27 pm	Evening	Overcast	ON	OFF	ON
2.8.18	9.03 to 9.12 am	Morning	Clear	OFF	ON	OFF
	9.13 to 9.22 am	Morning	Clear	ON	ON	OFF
	9.25 to 9.35 am	Morning	Clear	OFF	OFF	OFF
	9.36 to 9.46 am	Morning	Clear	ON	OFF	OFF
2.16.18	8.32 to 8.43 am	Morning	Clear	ON	OFF	OFF
	8.43 to 8.44 am	Morning	Clear	ON	OFF	ON
	8.45-8.57 am	Morning	Clear	ON	OFF	OFF
	8.57 to 9.06 am	Morning	Clear	OFF	ON	OFF
	9.07 to 9.15 am	Morning	Clear	ON	ON	OFF
	9.15 to 9.23 am	Morning	Clear	ON	ON	ON
	9.24 to 9.28 am	Morning	Clear	ON	ON	OFF
	9.29 to 9.32 am	Morning	Clear	OFF	ON	OFF
2.18.18	11.03 to 11.08 am	Morning	Clear	OFF	ON	OFF
	11.09 to 11.13 am	Morning	Clear	ON	ON	OFF
	11.15 to 11.19 am	Morning	Clear	ON	OFF	OFF
	11.22 to 11.27 am	Morning	Clear	ON	OFF	ON
	11.29 to 11.33 am	Morning	Clear	ON	ON	ON
	11.35 to 11.40 am	Morning	Clear	OFF	ON	ON
	11.40 to 11.45 am	Morning	Clear	ON	OFF	OFF
	11.46 to 11.51 am	Morning	Clear	ON	OFF	ON
	11.51 to 11.58 am	Morning	Clear	OFF	ON	ON
	11.59 to 12.05 am	Morning	Clear	ON	ON	ON

The limits established in the IEEE Std. 519 and 1457 take two important points in the power system as reference: the point of common coupling (PCC), which is the point where a local electrical power system (EPS) is connected to an area EPS, and the point of distributed resources (DR) connection, which is the point where a DR unit is electrically connected. In case of our system, the grid interconnection is depicted in Fig. 4.10:

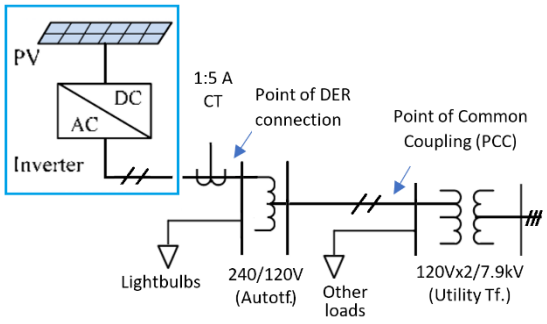

Figure 4.10: Simplified diagram of the grid interconnection

For the case of voltage, the measurements have been taken at the point of DER connection, that is at the 240 V RMS side of the autotransformer. The standards ask to consider the voltage at the PCC, which is equivalent to transforming the measured voltages to the 120V side. If the losses between the autotransformer and the PCC are neglected, it would be the same to measure harmonics at the DER and take 240 as the reference as to measure at the PCC and take 120V instead. In the case of currents, however, one must consider the equivalent of the maximum load current at the PCC, transformed to the point of DER.

Considering the voltage harmonic limits from the IEEE Std. 519, Tables 4.9 to 4.16 show the values for AC voltage measured at the inverter output under different conditions of PV source and Load.

Discussion of Results:

Inverter AC Voltage:

- PV OFF, load OFF. Dates: 9/20/2017 15:21-15:43, Clear afternoon

Table 4.9: Experimental results for RMS Voltage V1.

	Percentage (%) of Vnom																								
Fund	V3 mag	V5 mag	V7 mag	V9 mag	V11 mag	V13 mag	V15 mag	V17 mag	V19 mag	V21 mag	V23 mag	V25 mag	V27 mag	V29 mag	V31 mag	V33 mag	V35 mag	V37 mag	V39 mag	V41 mag	V43 mag	V45 mag	V47 mag	V49 mag	THD
100	1.16	1.57	1.49	0.98	1.22	1.63	0.61	0.30	0.78	0.59	0.56	0.25	0.07	0.23	0.06	0.04	0.06	0.04	0.04	0.05	0.04	0.04	0.05	0.02	3.61
100	1.17	1.57	1.48	0.98	1.19	1.61	0.62	0.29	0.78	0.60	0.56	0.25	0.07	0.24	0.06	0.04	0.06	0.04	0.04	0.06	0.04	0.04	0.05	0.02	3.59
100	1.18	1.58	1.48	0.98	1.19	1.61	0.62	0.29	0.79	0.60	0.57	0.25	0.07	0.25	0.06	0.04	0.06	0.04	0.04	0.06	0.04	0.04	0.06	0.02	3.60
100	1.33	1.32	1.29	0.86	1.16	1.34	0.48	0.27	0.72	0.52	0.50	0.31	0.18	0.26	0.03	0.07	0.06	0.06	0.06	0.03	0.03	0.02	0.04	0.02	3.27
100	1.36	1.34	1.28	0.87	1.16	1.34	0.47	0.27	0.72	0.51	0.51	0.30	0.17	0.27	0.03	0.08	0.06	0.05	0.05	0.03	0.02	0.01	0.04	0.02	3.29
100	1.34	1.33	1.29	0.86	1.18	1.34	0.46	0.27	0.72	0.51	0.48	0.31	0.17	0.25	0.02	0.07	0.05	0.06	0.06	0.03	0.03	0.02	0.04	0.02	3.27
Limits	5	5	5	5	5	5	5	5	5	5	5	5	5	5	5	5	5	5	5	5	5	5	5	5	8
Viols.	**0**	**0**	**0**	**0**	**0**	**0**	**0**	**0**	**0**	**0**	**0**	**0**	**0**	**0**	**0**	**0**	**0**	**0**	**0**	**0**	**0**	**0**	**0**	**0**	**0**

- PV ON, load OFF. Dates: 9/20/2017 18:53-18:58 and 10/10/2017 11:20-11:29, Clear evening.

Table 4.10: Experimental results for RMS Voltage V1.

	Percentage (%) of Vnom																								
Fund	V3 mag	V5 mag	V7 mag	V9 mag	V11 mag	V13 mag	V15 mag	V17 mag	V19 mag	V21 mag	V23 mag	V25 mag	V27 mag	V29 mag	V31 mag	V33 mag	V35 mag	V37 mag	V39 mag	V41 mag	V43 mag	V45 mag	V47 mag	V49 mag	THD
100	1.12	1.69	1.53	0.86	1.09	1.72	0.60	0.25	0.78	0.68	0.81	0.26	0.14	0.49	0.11	0.16	0.05	0.13	0.06	0.02	0.04	0.01	0.01	0.03	3.73
100	1.11	1.69	1.52	0.89	1.12	1.74	0.63	0.25	0.76	0.66	0.82	0.23	0.10	0.47	0.08	0.16	0.07	0.13	0.03	0.02	0.04	0.01	0.01	0.03	3.74
100	1.11	1.70	1.50	0.92	1.14	1.77	0.60	0.26	0.76	0.64	0.81	0.21	0.12	0.50	0.13	0.18	0.08	0.13	0.04	0.01	0.03	0.01	0.02	0.03	3.76
100	1.11	1.69	1.50	0.95	1.16	1.81	0.53	0.29	0.75	0.61	0.76	0.18	0.11	0.48	0.14	0.16	0.06	0.13	0.05	0.03	0.04	0.01	0.02	0.03	3.76
100	1.12	1.70	1.50	0.97	1.17	1.85	0.46	0.32	0.75	0.62	0.72	0.18	0.10	0.46	0.11	0.15	0.05	0.12	0.04	0.02	0.04	0.01	0.02	0.02	3.77
100	1.13	1.71	1.51	0.95	1.16	1.82	0.44	0.32	0.74	0.65	0.73	0.17	0.11	0.45	0.13	0.14	0.05	0.14	0.04	0.02	0.04	0.01	0.02	0.03	3.76
100	1.13	1.08	1.12	0.87	1.01	1.25	0.42	0.27	0.52	0.53	0.46	0.35	0.19	0.29	0.02	0.11	0.04	0.05	0.07	0.05	0.03	0.02	0.03	0.02	2.90
100	1.12	1.08	1.12	0.86	1.02	1.25	0.41	0.28	0.52	0.53	0.46	0.36	0.19	0.31	0.02	0.11	0.05	0.05	0.07	0.05	0.03	0.02	0.03	0.02	2.90
100	1.13	1.08	1.13	0.86	1.01	1.26	0.42	0.28	0.52	0.54	0.46	0.36	0.20	0.30	0.02	0.11	0.05	0.05	0.07	0.05	0.03	0.02	0.03	0.02	2.90
100	1.14	1.07	1.13	0.85	1.01	1.25	0.41	0.28	0.54	0.52	0.46	0.34	0.18	0.30	0.02	0.09	0.06	0.05	0.06	0.05	0.03	0.02	0.03	0.02	2.90
100	1.16	1.09	1.12	0.84	1.00	1.26	0.41	0.28	0.54	0.52	0.46	0.33	0.18	0.29	0.02	0.09	0.06	0.05	0.06	0.05	0.03	0.02	0.03	0.02	2.91
100	1.18	1.09	1.13	0.86	1.03	1.28	0.42	0.30	0.54	0.53	0.45	0.34	0.19	0.28	0.04	0.09	0.04	0.04	0.07	0.05	0.03	0.01	0.03	0.02	2.94
Limits	5	5	5	5	5	5	5	5	5	5	5	5	5	5	5	5	5	5	5	5	5	5	5	5	8
Viols.	**0**	**0**	**0**	**0**	**0**	**0**	**0**	**0**	**0**	**0**	**0**	**0**	**0**	**0**	**0**	**0**	**0**	**0**	**0**	**0**	**0**	**0**	**0**	**0**	**0**

- PV ON, load ON. Dates: 10/17/2017 11:42-15:55 Overcast and Scattered clouds

Table 4.11: Experimental results for RMS Voltage V1.

	Percentage (%) of Vnom																							
Fund	V3 mag	V5 mag	V7 mag	V9 mag	V11 mag	V13 mag	V15 mag	V17 mag	V19 mag	V21 mag	V23 mag	V25 mag	V27 mag	V29 mag	V31 mag	V33 mag	V35 mag	V37 mag	V39 mag	V41 mag	V43 mag	V45 mag	V47 mag	V49 mag	THD
100	1.36	1.38	1.26	0.89	1.09	1.28	0.44	0.24	0.67	0.46	0.44	0.20	0.14	0.20	0.03	0.05	0.04	0.06	0.05	0.03	0.01	0.02	0.03	0.01	3.20
100	1.34	1.36	1.26	0.90	1.08	1.27	0.42	0.21	0.67	0.45	0.44	0.20	0.16	0.20	0.03	0.04	0.04	0.06	0.05	0.03	0.01	0.02	0.03	0.01	3.17
100	1.34	1.34	1.27	0.89	1.06	1.27	0.42	0.21	0.67	0.45	0.44	0.20	0.16	0.20	0.03	0.05	0.04	0.06	0.05	0.03	0.01	0.02	0.03	0.01	3.17
100	1.36	1.40	1.29	0.89	1.13	1.31	0.43	0.23	0.68	0.44	0.44	0.20	0.13	0.20	0.03	0.04	0.04	0.07	0.05	0.02	0.01	0.02	0.03	0.01	3.24
100	1.38	1.39	1.29	0.90	1.13	1.32	0.43	0.23	0.68	0.44	0.44	0.20	0.13	0.20	0.02	0.04	0.04	0.07	0.05	0.03	0.01	0.02	0.03	0.01	3.26
100	1.38	1.38	1.29	0.89	1.12	1.31	0.44	0.23	0.68	0.44	0.46	0.21	0.13	0.20	0.02	0.05	0.04	0.06	0.05	0.03	0.01	0.02	0.03	0.01	3.25
100	1.00	1.30	1.22	0.83	0.88	1.09	0.42	0.22	0.51	0.41	0.37	0.27	0.13	0.19	0.03	0.02	0.06	0.03	0.04	0.04	0.03	0.02	0.02	0.01	2.79
100	1.00	1.31	1.22	0.84	0.90	1.09	0.42	0.23	0.51	0.42	0.36	0.26	0.13	0.20	0.03	0.02	0.05	0.03	0.04	0.04	0.03	0.02	0.02	0.01	2.80
100	0.99	1.29	1.21	0.85	0.89	1.10	0.42	0.22	0.52	0.42	0.35	0.26	0.15	0.20	0.02	0.02	0.05	0.04	0.04	0.04	0.02	0.03	0.03	0.01	2.79
100	0.98	1.29	1.23	0.84	0.91	1.12	0.42	0.21	0.54	0.42	0.39	0.29	0.15	0.21	0.03	0.02	0.06	0.04	0.04	0.04	0.02	0.03	0.02	0.01	2.83
100	0.99	1.32	1.24	0.85	0.94	1.15	0.42	0.23	0.54	0.43	0.38	0.30	0.16	0.21	0.02	0.02	0.06	0.04	0.04	0.04	0.02	0.02	0.02	0.01	2.87
100	0.99	1.30	1.23	0.85	0.91	1.13	0.42	0.21	0.53	0.43	0.37	0.29	0.15	0.23	0.03	0.02	0.06	0.04	0.04	0.03	0.02	0.03	0.03	0.01	2.84
Limits	5	5	5	5	5	5	5	5	5	5	5	5	5	5	5	5	5	5	5	5	5	5	5	5	8
Viols.	**0**	**0**	**0**	**0**	**0**	**0**	**0**	**0**	**0**	**0**	**0**	**0**	**0**	**0**	**0**	**0**	**0**	**0**	**0**	**0**	**0**	**0**	**0**	**0**	**0**

- PV OFF, load ON. Dates: 7/12/2017 16:35-16:48 Overcast

Table 4.12: Experimental results for RMS Voltage V1.

	Percentage (%) of Vnom																							
Fund	V3 mag	V5 mag	V7 mag	V9 mag	V11 mag	V13 mag	V15 mag	V17 mag	V19 mag	V21 mag	V23 mag	V25 mag	V27 mag	V29 mag	V31 mag	V33 mag	V35 mag	V37 mag	V39 mag	V41 mag	V43 mag	V45 mag	V47 mag	V49 mag	THD
100	1.10	1.01	1.53	1.03	1.11	1.45	0.61	0.24	0.59	0.60	0.40	0.28	0.06	0.16	0.01	0.07	0.06	0.01	0.03	0.01	0.04	0.01	0.02	0.03	3.22
100	1.10	1.00	1.52	1.04	1.10	1.45	0.61	0.24	0.59	0.61	0.40	0.28	0.06	0.15	0.01	0.06	0.06	0.01	0.03	0.01	0.04	0.01	0.02	0.03	3.21
100	1.10	1.00	1.52	1.03	1.12	1.46	0.61	0.25	0.59	0.62	0.40	0.28	0.06	0.15	0.01	0.06	0.06	0.01	0.03	0.01	0.04	0.01	0.02	0.03	3.22
100	1.10	1.02	1.53	1.02	1.11	1.46	0.60	0.25	0.59	0.59	0.40	0.27	0.07	0.16	0.01	0.06	0.05	0.01	0.03	0.01	0.04	0.01	0.02	0.03	3.23
100	1.09	1.03	1.52	1.03	1.10	1.46	0.60	0.25	0.59	0.61	0.40	0.28	0.07	0.16	0.01	0.06	0.05	0.01	0.02	0.01	0.04	0.01	0.02	0.03	3.22
100	1.09	1.03	1.52	1.03	1.10	1.45	0.60	0.25	0.60	0.61	0.40	0.28	0.07	0.16	0.01	0.06	0.05	0.01	0.03	0.01	0.04	0.01	0.02	0.03	3.22
100	1.08	1.05	1.51	1.01	1.11	1.45	0.58	0.25	0.59	0.60	0.39	0.27	0.07	0.16	0.01	0.06	0.05	0.01	0.03	0.01	0.04	0.01	0.01	0.02	3.21
100	1.11	1.01	1.52	1.02	1.10	1.43	0.59	0.24	0.58	0.60	0.40	0.26	0.06	0.16	0.01	0.06	0.05	0.02	0.02	0.01	0.03	0.01	0.02	0.02	3.20
100	1.10	1.03	1.52	1.03	1.09	1.42	0.59	0.24	0.58	0.60	0.40	0.27	0.06	0.15	0.01	0.06	0.05	0.01	0.03	0.01	0.03	0.01	0.02	0.02	3.20
Limits	5	5	5	5	5	5	5	5	5	5	5	5	5	5	5	5	5	5	5	5	5	5	5	5	8
Viols.	**0**	**0**	**0**	**0**	**0**	**0**	**0**	**0**	**0**	**0**	**0**	**0**	**0**	**0**	**0**	**0**	**0**	**0**	**0**	**0**	**0**	**0**	**0**	**0**	**0**

Observations

- At no point there is violation in the voltage limits under any of the previous conditions of operation of our system. All the values recorded are within the limits of the IEEE Std. 519.
- The voltage that comes from the bulk grid is nearly the same as the one that goes to the inverter and the load.
- In the case of the PV module turned off and no loads, the PV voltage measured is the same as the one coming from the main grid. For that case, we see there are still harmonics present, which can come from the grid and from noise affecting our data acquisition system.
- Under the same operating conditions, there is a change in the THD recorded at different times of the day.
- The biggest voltage harmonics recorded for our system lay in the interval between the 3^{rd} and 23^{rd} order-component.
- Out of the cases reviewed, the minimum THD corresponds to the operation condition for PV ON and load ON. This could imply the module is contributing to a better voltage filtering and regulation.

Current C: current coming from the main grid

Case A: Reference conditions for a normal distribution system

Table 4.13: Reference conditions for Imax at PCC, case 1.

Capacity of Utility Transformer	25 kVA
Inominal at PCC	104.17 A
Maximum load	75%
Imax at PCC	78.13 A
Imax Eq. at Point of DER	39.06 A
Imax Eq. at CT	7.51 A

- PV OFF, load OFF: would only measure noise. Not included here.
- Load ON, PV OFF: Base condition. Clear morning

Table 4.14: Experimental results for RMS Current C.

	A RMS	Percentage (%) of Imax						
PC Local Time	I Fund	I Fund	C I 3 mag	C I 5 mag	C I 7 mag	C I 9 mag	C I 11 mag	C I 13 mag
2/16/2018 16:59	0.99	13.17	0.11	0.23	0.20	0.14	0.16	0.20
2/16/2018 17:00	0.99	13.17	0.10	0.23	0.20	0.15	0.16	0.21
2/16/2018 17:03	0.99	13.18	0.11	0.23	0.20	0.14	0.16	0.19
2/16/2018 17:05	0.99	13.17	0.10	0.22	0.19	0.14	0.17	0.22
	Limits		4	4	4	4	2	2
	Violations		0	0	0	0	0	0
	Average		0.10	0.23	0.20	0.14	0.16	0.20

For the other cases, the harmonics evaluated here are those measured minus the contribution from the base condition.

- Load OFF, PV ON. Clear morning

Table 4.15: Experimental results for RMS Current C.

	A RMS	Injection in Percentage (%) of Imax						
PC Local Time	I Fund	I Fund	C I 3 mag	C I 5 mag	C I 7 mag	C I 9 mag	C I 11 mag	C I 13 mag
2/18/2018 11:55	0.79	10.55	0.75	0.46	0.21	0.25	0.19	0.16
2/18/2018 11:57	0.80	10.64	0.73	0.44	0.20	0.24	0.18	0.16
2/18/2018 11:58	0.80	10.61	0.71	0.44	0.21	0.25	0.19	0.17
2/18/2018 12:00	0.80	10.68	0.72	0.43	0.20	0.25	0.19	0.17
	Limits		4	4	4	4	2	2
	Violations		0	0	0	0	0	0

- Load ON, PV ON. Clear morning

Table 4.16: Experimental results for RMS Current C.

	A RMS	Injection in Percentage (%) of Imax						
PC Local Time	I Fund	I Fund	C I 3 mag	C I 5 mag	C I 7 mag	C I 9 mag	C I 11 mag	C I 13 mag
2/16/2018 9:25	0.76	10.10	0.28	0.20	0.28	0.24	0.15	0.19
2/16/2018 9:26	0.72	9.63	0.31	0.22	0.28	0.25	0.18	0.22
2/16/2018 9:27	0.72	9.56	0.30	0.23	0.26	0.26	0.20	0.27
2/16/2018 9:28	0.76	10.13	0.28	0.20	0.27	0.24	0.17	0.26
	Limits		4	4	4	4	2	2
	Violations		0	0	0	0	0	0

Observations:

- One of the most noticeable things when evaluating the harmonics according to the IEEE Std. 1547 is that the harmonics are considered as a percentage of a maximum load. Depending on this load, the results vary.
- For this first case, with a reference under normal conditions of a PCC and described in Table 4.13, there are no violations of the limits whether the PV system and load are ON or OFF.
- The IEEE Stds. 519 and 1547 asks to consider the percentage of harmonic injection, so it is necessary to describe first the conditions at the PCC without the DER in order to discriminate how much of the harmonics that are measured after the interconnection actually come from the microgrid.

Case B: Reference conditions for single load in a distribution system

Table 4.17: Reference conditions for Imax at PCC, case 2.

Capacity of Utility Transformer	5 kVA
Inominal at PCC	20.83 A
Maximum load	48.4%
Imax at PCC	10.08 A
Imax Eq. at Point of DER	5.04 A
Imax Eq. at CT	0.97 A

- Load ON, PV OFF. Clear morning

Table 4.18: Experimental results for RMS Current C.

	A RMS	Percentage (%) of Imax						
PC Local Time	I Fund	I Fund	C I 3 mag	C I 5 mag	C I 7 mag	C I 9 mag	C I 11 mag	C I 13 mag
2/16/2018 16:59	0.99	102	0.83	1.79	1.52	1.11	1.26	1.51
2/16/2018 17:00	0.99	102	0.80	1.76	1.51	1.15	1.27	1.65
2/16/2018 17:03	0.99	102	0.85	1.75	1.56	1.07	1.20	1.49
2/16/2018 17:05	0.99	102	0.75	1.67	1.48	1.07	1.28	1.67
	Limits		4	4	4	4	2	2
	Violations		0	0	0	0	0	0
	Average		0.81	1.74	1.52	1.10	1.25	1.58

For the other cases, the harmonics evaluated here are those measured minus the contribution from the base condition.

- Load OFF, PV ON. Clear morning

Table 4.19: Experimental results for RMS Current C.

	A RMS	Injection in Percentage (%) of Imax						
PC Local Time	I Fund	I Fund	C I 3 mag	C I 5 mag	C I 7 mag	C I 9 mag	C I 11 mag	C I 13 mag
2/18/2018 11:55	0.79	81.64	5.78	3.58	1.62	1.93	1.45	1.27
2/18/2018 11:57	0.80	82.30	5.66	3.37	1.52	1.88	1.41	1.24
2/18/2018 11:58	0.80	82.10	5.50	3.37	1.60	1.97	1.50	1.29
2/18/2018 12:00	0.80	82.61	5.59	3.34	1.58	1.93	1.47	1.29
	Limits		4	4	4	4	2	2
	Violations		4	0	0	0	0	0

- Load ON, PV ON. Clear morning

Table 4.20: Experimental results for RMS Current C.

	A RMS	Injection in Percentage (%) of Imax						
PC Local Time	I Fund	I Fund	C I 3 mag	C I 5 mag	C I 7 mag	C I 9 mag	C I 11 mag	C I 13 mag
2/16/2018 9:25	0.76	78.17	2.17	1.58	2.14	1.84	1.19	1.47
2/16/2018 9:26	0.72	74.49	2.39	1.72	2.16	1.93	1.41	1.68
2/16/2018 9:27	0.72	73.98	2.33	1.81	2.04	2.00	1.55	2.06
2/16/2018 9:28	0.76	78.40	2.13	1.52	2.05	1.87	1.31	1.99
	Limits		4	4	4	4	2	2
	Violations		0	0	0	0	0	1

Observations:

- For the case of currents, the base scenario is when the main power grid provides all the current to our load. That happens when the load is turned ON but the PV system is OFF.
- In that case scenario, there is no violation of the limits for both cases A and B, but we can notice high percentage in the 11^{th}, and 13^{th}-order harmonics when compared to their respective limits. This is the background current, which is deducted from the other measurements.
- Table 4.19 shows violations at the 3rd-order harmonics, and values very close to the limits at the 5th, 11^{th}, and 13^{th}-order. Notice that both Tables 4.15 and 4.19 represent the same scenario: The Load is OFF and the PV Source ON, so we are injecting all the current generated into the mains.
- Under such scenario, the records show violations only when the maximum current of at the PCC is not high enough to mitigate the contribution of the harmonics injected (Case B).

- When both the load of the system is ON and so is the PV source, we can only see violations in 13th order harmonics.
- Cases in which the recorded current was too low have not been included in this article, to avoid considering high percentages of noise in our computations.
- The logical conclusion is that there is a minimum current at the PCC for which it is permissible to connect this DER to the main grid in compliance with the IEEE Std. 1547.

- Contribution of distorting loads

The values in Tables 4.12 to 4.19 were recorded during periods where other possibly distorting loads were connected to the grid. To isolate the effect of such loads, namely computer equipment and fluorescent lights operating in the lab, the following contrast is presented

Table 4.21: Experimental results for RMS Current C

Operating conditions		Percentage (%) of Imax					
		C I 3 mag	C I 5 mag	C I 7 mag	C I 9 mag	C I 11 mag	C I 13 mag
Case 1	Lights OFF	6.18	5.06	2.99	2.89	2.53	2.78
PV ON	Lights ON	6.25	5.01	3.01	2.94	2.63	2.77
Load OFF	**Difference**	**0.07**	**-0.05**	**0.02**	**0.05**	**0.10**	**-0.01**
Case 2	Lights OFF	0.51	1.26	1.40	0.83	1.04	1.42
PV ON	Lights ON	0.51	1.26	1.40	0.83	1.07	1.41
Load OFF	**Difference**	**0.00**	**0.00**	**0.00**	**0.00**	**0.02**	**-0.01**
Case 3	Lights OFF	2.94	3.15	3.40	2.89	2.60	3.13
PV ON	Lights ON	2.97	3.30	3.51	2.92	2.54	3.28
Load OFF	**Difference**	**0.04**	**0.15**	**0.11**	**0.03**	**-0.05**	**0.15**
Average	**Difference**	**0.03**	**0.03**	**0.04**	**0.03**	**0.02**	**0.04**

The values in Table 4.21 correspond to the average of several measurements taken the same day before and after turning the fluorescent lights and computers ON. The

maximum current taken as common reference was chosen to be 1A. It can be noticed that the difference between both scenarios is very small and their contribution for the type of loads used in the experiment can be neglected in our analysis. In some cases, there is a negative difference, which can be explained by some compensation between these inductive loads and the capacitive component of the bulk power grid.

Case C – Minimum permissible current criteria.

Taking the previous considerations, one can figure out the minimum permissible current at the PCC that would allow us to interconnect this DER to the grid in compliance with the limits in the IEEE Std. 1543-2013.

For the different operation scenarios, the highest harmonics recordings are shown in table 4.22. Knowing the harmonics limits as a percentage of the maximum load current at the PCC, one can calculate the minimum load current necessary to comply with the standard.

Table 4.22: Experimental results for RMS Current C.

	Max. Harmonic detected, A RMS					
	C I 3	C I 5	C I 7	C I 9	C I 11	C I 13
Max. Harm.	0.06	0.03	0.02	0.02	0.02	0.02
Min. Imax	1.40	0.87	0.52	0.56	0.96	1.13

Out of the previous reference currents, the highest one was chosen as the minimum limit. This corresponds to 1.40 A RMS at the CT side, which equates to 7.28 A RMS at the point of DER connection, and 14.56 A at the PCC. Due to harmonic distortion, our DER system would be limited to be connected to a Power Grid that feeds at least 14.56 A at the PCC to comply with the harmonic injection limits permissible. See table 4.23.

Table 4.23: Experimental results for RMS Current C.

A RMS	Injection in Percentage (%) of Imax					
I Fund	C I 3	C I 5	C I 7	C I 9	C I 11	C I 13
1.40	3.98	2.46	1.49	1.59	1.36	1.60
Limit	4	4	4	4	2	2

4.2.2.Voltage variations

To analyze voltage, the RMS measurements taken by the Arbiter System DAQ have been used. A MATLAB program was developed to analyze voltage limits. For several conditions of Load and PV Source during the day, no violations were shown. The maximum recorded values reflect the settings configured at the SolarMax 2000 Inverter, which have been compared to the permissible limits in the IEEE Std. 1547-2014.

Table 4.24: Experimental results for inverter AC Voltage.

	Pre-configured		Meas.	IEEE 1547- 2014	
	Limit	t max	Vmax	Limit	tmax
Vmax	264	0.2s	-	>=288	0.16s
			-	>264	1-13s
Vmin	196	1.5s	-	<211	2-21s
			-	<144	1-11s
			-	<108	0.16s
Vmax	253	600s	253	264	Cont.
Vmin	-	-	223	211	Cont.

Notice that the measured voltages comply with the continuous operation limits of the Standard (see Table 12, two last rows). However, the pre-configured limit voltages do not comply with the Min or Max voltage limits under 0.16 seconds, or with the 144 Min voltage limit under 11 seconds. To better assess the effect such violations would have on the equipment to be fed by our microgrid, we superpose the allowable operation limits to the ITI/CBEMA curve. The ITI acceptability curve is a reference of the

maximum voltage deviations generally accepted by computer-type equipment manufacturers.

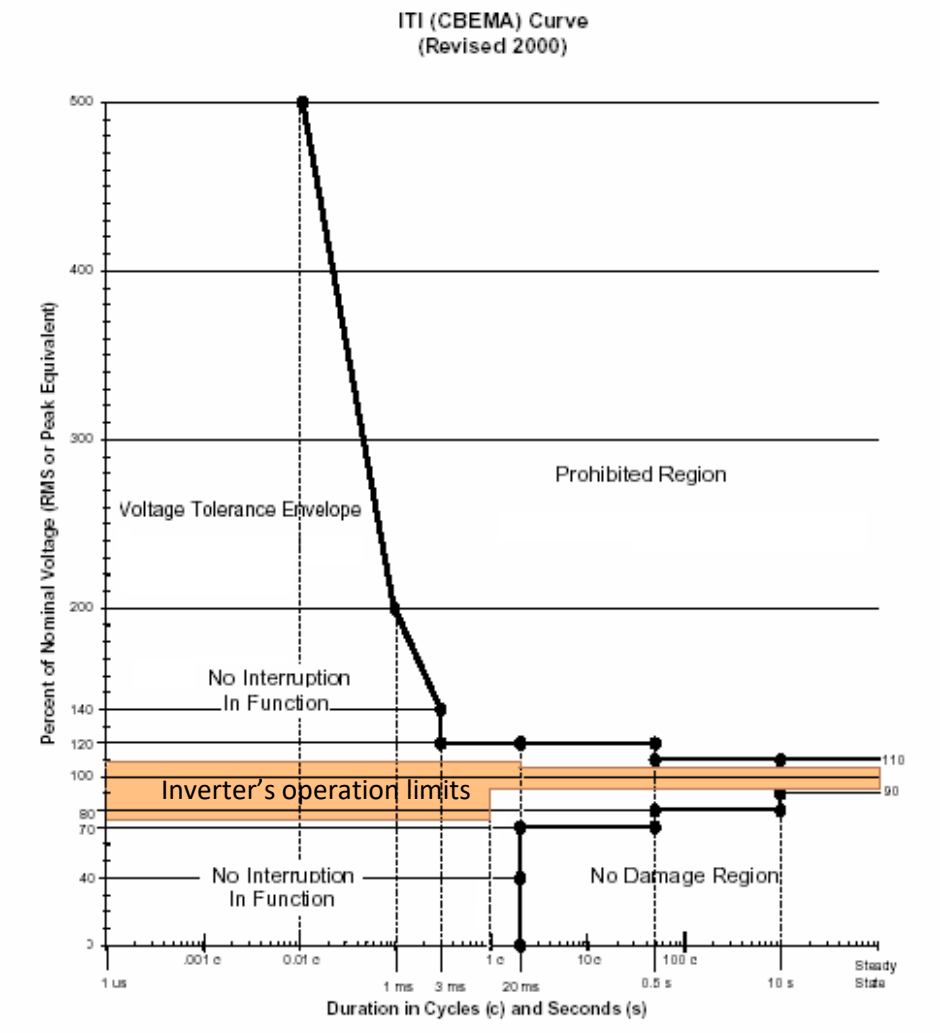

Figure 4.11: Operation limits of the module on the ITI/CBEMA curve.

As it can be seen in Fig. 4.11, the inverter operation limits lay within the region of functional state of most Information Technology Equipment. Thus, it is fair to assume that most electronic-based equipment should not be affected by the microgrid operation despite the discrepancies with some AC voltage limits in the IEEE 1547. Different

equipment, however, may have different voltage requirements, so it is always recommended to consult the information given by the manufacturer.

CHAPTER 5: CONCLUSIONS AND FUTURE WORK

5.1. Conclusions

Several conclusions have been obtained from this project. From the initial set of parameters for data measuring, a large amount of information was recorded but only part of it has been presented here. A photovoltaic system working with a maximum power point tracking (MPPT) algorithm is a system with high variability, for both design and atmospheric conditions. In addition, changes in the conditions of the power grid to which is connected also affect the system and the interaction between microgrid and bulk power grid needs to be evaluated. Therefore, the relevant experiments had to be taken under similar conditions, and the changes to be evaluated should be the sole difference between each round of experiments. For example, clear weather gives less variability in solar power. In consequence, the best data was obtained during clear weather days, before and after changing the conditions that needed to be contrasted.

By observing the different records for voltage harmonics of this system, we notice that it stays under the limits of the IEEE Std. 519 – "Recommended Practice and Requirements for Harmonic Control in Electric Power Systems" under any condition previously tested: load ON or OFF, and PV source ON or OFF. Therefore, we can say the operation is successfully complying with the standard for nominal voltage conditions in the grid. Regarding the voltage variations, the control settings of the device also allow that even when the local power grid is experiencing overvoltage or under-voltage conditions, the photovoltaic (PV) system will stay within its previously configured limits, and if the grid is too far from these limits, the system will just be disconnected. The

configuration tested generally complies with the voltage magnitude limits of the IEEE Std. 1547 – "Standard for Interconnecting Distributed Resources with Electric Power Systems", and for those specific periods when it doesn't, a further analysis of the ITI/CBEMA curve shows us that the system operates in the safe zone for most information technology equipment. In any case, inverter configuration settings can be changed for commercial PV applications according to the specific country's regulation, and with the special manufacturer's recommendations for critical equipment being fed.

The experiments performed for current harmonic analysis have shown the appropriate power quality of this microgrid working in grid-connected mode. It is noticeable that under common conditions for a distribution network, the harmonics represent just a few percentages of the maximum load at the Point of Common Coupling, which are the imposed limits according to the IEEE Std. 1547. Consequently, the evaluated module complies with the power quality requirement. If the maximum load was low enough, which happens for a very weak system at the point of common coupling (PCC) or for the case of a system only feeding its own load, the harmonic injection represents a limit to the grid integration.

Given that the harmonics recorded are consistent for the same conditions of operation, a simple design criterion to check the impact in the grid power quality of a given microgrid has been applied. The procedure consists of first taking records of the background harmonics and possible distorting loads, and then deduct them from the measurements for a specific microgrid with distributed energy resources (DER) when it is connected. That way, it can be determined how much the minimum load current needs to be at the PCC for the microgrid to be connected in a proposed location in compliance with the power quality requirements. The tests have been performed at the user's final

location but can also be run in the manufacturer's laboratory because the DER interconnection standard evaluates the contribution of harmonics injected to the bulk grid, and not the overall harmonics at that point.

5.2. Future work

One of the first outcomes of this project has been to learn the set-up of the microgrid system present in the Power Systems Automation and Control Laboratory, and its relevant data acquisition devices. The present module can be further used to study the variability of the energy produced under different conditions and the interaction with other types of loads. New studies can also assess the impact of different protection and control strategies applied to this microgrid as well as the interaction with the local power grid.

Another future goal is to perform the modeling and simulation of this microgrid system under different operating scenarios. By developing simple simulations using MATLAB's Simulink, or including studies performed in other software such as WinIGS and OpenDSS, it can be easier to test different conditions to describe the factors that may also limit the integration to the local power system, as well as to propose strategies to improve the overall grid power quality.

5.3. Closing thoughts

Some authors have identified that the IEEE Std. 1547 is constantly under revision, whereas others have performed mostly theoretical studies about the different national regulations for the integration of distributed energy resources into the bulk grid. The proposed study can be taken as a practical guide for anyone who would like to assess the impact of a specific design of an inverter and microgrid in the local power grid, and the implications in the power quality.

APPENDIX A: CURRENT TRANSFORMERS CALIBRATION TEST

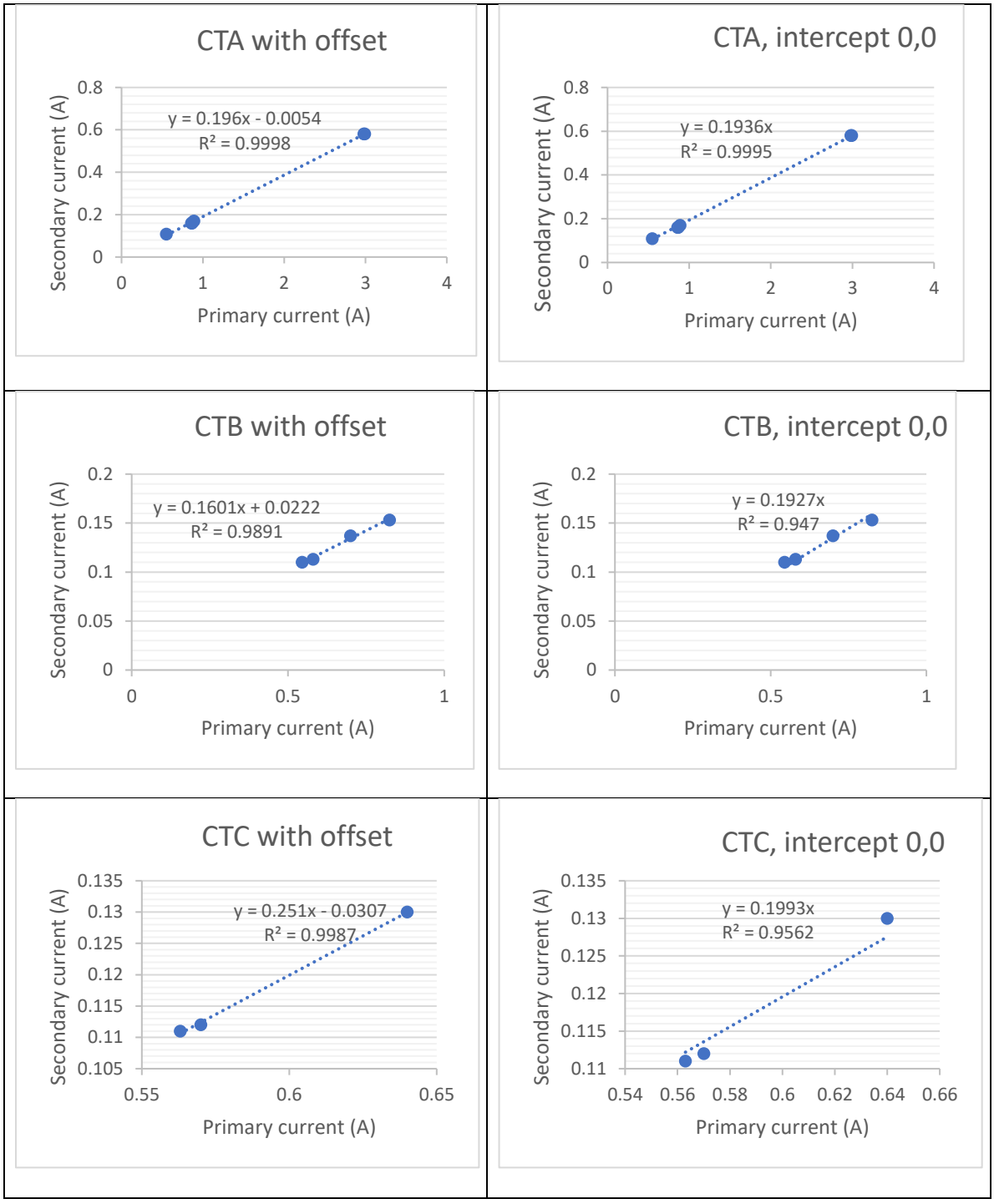

Figure A.1: Ratio of the AC current transformers.

Note: Using Excel's linear regression, an R-squared closer to 1 indicates a better fit to the equation.

APPENDIX B: CODE IMPLEMENTED FOR HARMONIC ANALYSIS

```
read_comtradefull
T = 1/Sample_rate;            % Sampling period is 8160 per sec
L = length(Rear_1_Grid);      % Length of signal
time9 = (0:1:L-1)*T;          % Discrete time vector, varies with each measurement
F=zeros(15,50);               %Initialize thd vector for freq
fix=L/24480;                  %how many "three-secs windows" do I have
%for yy=1:1:1
for yy=1:1:fix
   Rear_1_GridI=Rear_1_Grid(24480*(yy-1)+1:24480*(yy));
   %Separates full 3 sec records for each one of those windows
   for m=1:1:15 %15 times 12 cycles
   %for m=1:1:1 %1 time 12 cycles
      %Different plots in different windows
      %1632 represents 12 cycles = 0.2 seconds*8160samples/s
      x=Rear_1_GridI(1632*(m-1)+1:1632*m);%just that period of 0.2 secs
      y=fft(x);
      Lx=length(x); %For those 12 cycles, redundant
            %iy=ifft(P1)
            %iy2=real(iy)
            %wiii=P1-iy2
      %Here starts the FFT method found on MATLAB exchange website
      P2 = abs(y/Lx); %Since FFT multiplies by *Lx, then I must divide by Lx.
      P1 = P2(1:Lx/2+1); %from element 1 to half+1 = only first half considered.
      P1(2:end-1) = 2*P1(2:end-1); %Second scale: must multiply by two to escalate. Ignores f0.
```

```
    f = Sample_rate*(0:(Lx/2))/Lx; %All frequencies 0 5 10 according to fft.
    phase=0;
    xabs=abs(x);
    minx=min(xabs);
    [M,iii]=min(xabs);
    yyy=(iii-1)*T; %yyy is the time stamp for that value, that is the closest to zero
        if x(iii+1)>x(iii)
           phase=yyy*2*pi*60;
        else
           phase=pi+yyy*2*pi*60;
        end
    P1rms=(sqrt(2)/2)*P1;
    n=zeros(1,50);
    %Grouping.
    for jj=1:1:50
       %position is 12jj+1, and the two 5hz contiguous
       a=((P1rms(12*jj))^2)+((P1rms(12*jj+1))^2)+((P1rms(12*jj+2))^2);
       %a=((P1(12*jj+1))^2);
       n(jj)=sqrt(a);
    end
    F(m,:)=n;%That "m" row will be the full result of n for this iteration
    %m-th collection of 12 cycles, 15 in total
    %Analyzed up to 50th harmonic only, column is harmonic number.
end
F %Frequency components for that period
Fvs=zeros(1,50);
```

```
    for nn=1:1:50
        %for each harmonic column
        sum=0;
        for o=1:1:15
            sum=sum+(F(o,nn))^2;
            %sums all the rows, that is all the samples
        end
        Fvs(nn)=sqrt(sum/15);
    end
    Fvs %this includes the summary of the very short time for that specific harmonic
    Fvs_100(yy,:)=Fvs*100/Fvs(1);
    THDvI=0;
    for nn=2:1:50
        THDvI=THDvI+(Fvs(nn)^2);
    end
    THDvTotal(yy)=(sqrt(THDvI));
    THDv_100(yy)=THDvTotal(yy)*100/Fvs(1);
end
THDvTotal
THDv_100
Fvs_100
```

APPENDIX C: CURRENT HARMONICS RECORDS

1. Reference conditions for a normal distribution system

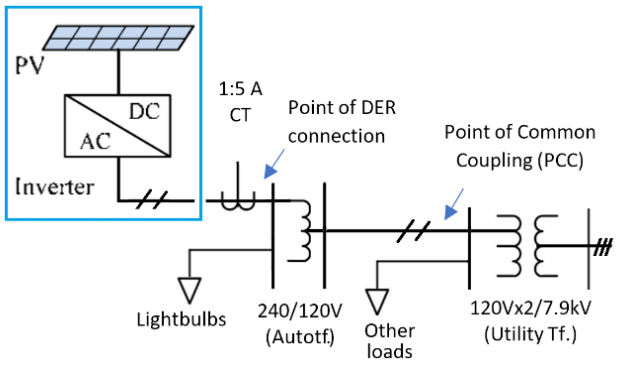

Figure C.1: Simplified diagram of the grid interconnection

Conditions:

Utility Transformer = 25 kVA. Inominal at PCC = $25x10^3/(120x2)$ = 104.17 A.

Consider Max. load 75%

Imax at PCC =78.13 A at 120V side (PCC) = 39.06 at 240V side (Point of DER) = 7.51 A at CT

A) Load OFF, PV ON: All current from PV to the grid.

Lights OFF

2.18.18, clear morning.

Table C.1: Experimental results for RMS current C

A RMS	Percentage (%) of Imax						
I Fund	I Fund	C I 3	C I 5	C I 7	C I 9	C I 11	C I 13
0.76	10.06	0.82	0.67	0.40	0.38	0.33	0.37
0.76	10.13	0.83	0.67	0.40	0.37	0.33	0.37
0.76	10.14	0.82	0.67	0.40	0.39	0.34	0.37
0.76	10.13	0.82	0.68	0.40	0.39	0.34	0.37

Lights ON

2.18.18, Clear morning

Table C.2: Experimental results for RMS current C

A RMS	Percentage (%) of Imax						
I Fund	I Fund	C I 3	C I 5	C I 7	C I 9	C I 11	C I 13
0.79	10.55	0.85	0.69	0.41	0.39	0.35	0.37
0.80	10.64	0.84	0.66	0.39	0.38	0.34	0.36
0.80	10.61	0.81	0.66	0.40	0.40	0.36	0.37
0.80	10.68	0.83	0.66	0.40	0.39	0.35	0.37

11.20.17, Clear morning

Table C.3: Experimental results for RMS current C

A RMS	Percentage (%) of Imax						
I Fund	I Fund	C I 3	C I 5	C I 7	C I 9	C I 11	C I 13
0.69	9.22	0.80	0.64	0.44	0.42	0.35	0.41
0.66	8.80	0.74	0.59	0.43	0.42	0.35	0.41
0.72	9.54	0.80	0.63	0.45	0.44	0.37	0.41
0.72	9.53	0.81	0.63	0.46	0.43	0.36	0.40
0.71	9.48	0.80	0.61	0.46	0.44	0.37	0.42

B) Load ON, PV OFF. Only grid feeds load.

Lights OFF

2.18.18, clear morning

Table C.4: Experimental results for RMS current C

A RMS	Percentage (%) of Imax						
I Fund	I Fund	C I 3	C I 5	C I 7	C I 9	C I 11	C I 13
0.99	13.14	0.07	0.17	0.18	0.11	0.14	0.19
0.99	13.14	0.07	0.17	0.19	0.11	0.14	0.19
0.99	13.15	0.07	0.17	0.19	0.11	0.14	0.19
0.99	13.14	0.07	0.17	0.19	0.11	0.14	0.19

Lights ON

2.18.18, clear morning

Table C.5: Experimental results for RMS current C

A RMS	Percentage (%) of Imax						
I Fund	I Fund	C I 3	C I 5	C I 7	C I 9	C I 11	C I 13
0.99	13.14	0.07	0.17	0.19	0.11	0.14	0.19
0.99	13.14	0.07	0.17	0.19	0.11	0.14	0.19
0.99	13.14	0.07	0.17	0.19	0.11	0.14	0.19
0.99	13.14	0.07	0.17	0.19	0.11	0.14	0.19

2.18.18, clear morning

Table C.6: Experimental results for RMS current C

A RMS	Percentage (%) of Imax						
I Fund	I Fund	C I 3	C I 5	C I 7	C I 9	C I 11	C I 13
0.99	13.16	0.07	0.17	0.19	0.11	0.14	0.19
0.99	13.16	0.07	0.17	0.19	0.11	0.14	0.19
0.99	13.16	0.07	0.17	0.19	0.11	0.14	0.19
0.99	13.16	0.07	0.17	0.18	0.11	0.14	0.19

2.18.18, clear morning

Table C.7: Experimental results for RMS current C

A RMS	Percentage (%) of Imax						
I Fund	I Fund	C I 3	C I 5	C I 7	C I 9	C I 11	C I 13
0.99	12.92	0.07	0.17	0.18	0.11	0.14	0.19
0.99	12.92	0.07	0.17	0.19	0.11	0.14	0.19
0.99	12.92	0.07	0.17	0.19	0.11	0.14	0.19
0.99	12.92	0.07	0.17	0.19	0.11	0.14	0.19

2.16.18, overcast afternoon

Table C.8: Experimental results for RMS current C

A RMS	Percentage (%) of Imax						
I Fund	I Fund	C I 3	C I 5	C I 7	C I 9	C I 11	C I 13
0.99	13.17	0.11	0.23	0.20	0.14	0.16	0.20
0.99	13.17	0.10	0.23	0.20	0.15	0.16	0.21
0.99	13.18	0.11	0.23	0.20	0.14	0.16	0.19
0.99	13.17	0.10	0.22	0.19	0.14	0.17	0.22

11.14.18, clear afternoon

Table C.9: Experimental results for RMS current C

A RMS	Percentage (%) of Imax						
I Fund	I Fund	C I 3	C I 5	C I 7	C I 9	C I 11	C I 13
0.96	12.80	0.23	0.28	0.43	0.34	0.42	0.49
0.97	12.85	0.21	0.28	0.41	0.35	0.40	0.48
0.97	12.88	0.20	0.27	0.41	0.35	0.39	0.48
0.97	12.94	0.20	0.27	0.42	0.36	0.39	0.47
0.98	13.02	0.17	0.26	0.41	0.36	0.41	0.50

C) Current from grid and PV. Load ON, PV On.

Current A

Lights OFF

2.18.18, clear morning

Table C.10: Experimental results for RMS current A

A RMS	Percentage (%) of Imax						
I Fund	I Fund	A I 3	A I 5	A I 7	A I 9	A I 11	A I 13
0.74	9.86	0.28	0.34	0.38	0.16	0.26	0.31
0.74	9.89	0.27	0.35	0.38	0.16	0.26	0.30
0.74	9.89	0.28	0.35	0.38	0.16	0.27	0.30
0.75	9.96	0.29	0.35	0.39	0.17	0.26	0.31

Lights ON

2.18.18, clear morning

Table C.11: Experimental results for RMS current A

A RMS	Percentage (%) of Imax						
I Fund	I Fund	A I 3	A I 5	A I 7	A I 9	A I 11	A I 13
0.75	10.02	0.27	0.35	0.38	0.15	0.27	0.30
0.76	10.11	0.27	0.34	0.39	0.17	0.26	0.31
0.76	10.13	0.29	0.34	0.40	0.18	0.26	0.32
0.77	10.28	0.30	0.33	0.39	0.19	0.25	0.31

11.20.17, clear morning

Table C.12: Experimental results for RMS current A

A RMS	Percentage (%) of Imax						
I Fund	I Fund	A I 3	A I 5	A I 7	A I 9	A I 11	A I 13
0.70	9.26	0.61	0.48	0.41	0.40	0.31	0.38
0.72	9.54	0.63	0.50	0.42	0.39	0.33	0.39
0.71	9.42	0.59	0.46	0.43	0.38	0.30	0.38
0.73	9.68	0.60	0.47	0.43	0.38	0.29	0.37
0.74	9.83	0.63	0.50	0.43	0.40	0.31	0.37

Current C:

Lights OFF

2.8.17, clear morning

Table C.13: Experimental results for RMS current C

A RMS	Percentage (%) of Imax						
I Fund	I Fund	C I 3	C I 5	C I 7	C I 9	C I 11	C I 13
0.90	12.02	0.27	0.28	0.33	0.31	0.39	0.40
0.91	12.11	0.27	0.28	0.34	0.31	0.39	0.41
0.91	12.15	0.26	0.27	0.33	0.31	0.38	0.40
0.91	12.11	0.27	0.28	0.32	0.31	0.38	0.41
0.91	12.12	0.26	0.27	0.33	0.31	0.38	0.39

2.16.18, clear morning

Table C.14: Experimental results for RMS current C

A RMS	Percentage (%) of Imax						
I Fund	I Fund	C I 3	C I 5	C I 7	C I 9	C I 11	C I 13
0.75	9.95	0.39	0.41	0.47	0.37	0.34	0.41
0.73	9.65	0.40	0.44	0.46	0.39	0.33	0.39
0.78	10.41	0.38	0.40	0.43	0.40	0.36	0.45

Lights ON

2.16.18, clear morning

Table C. 15: Experimental results for RMS current C

A RMS	Percentage (%) of Imax						
I Fund	I Fund	C I 3	C I 5	C I 7	C I 9	C I 11	C I 13
0.76	10.10	0.38	0.43	0.47	0.38	0.32	0.39
0.72	9.63	0.41	0.45	0.48	0.39	0.34	0.42
0.72	9.56	0.41	0.46	0.46	0.40	0.36	0.47
0.76	10.13	0.38	0.42	0.46	0.38	0.33	0.46

2. Reference conditions for single load in distribution system

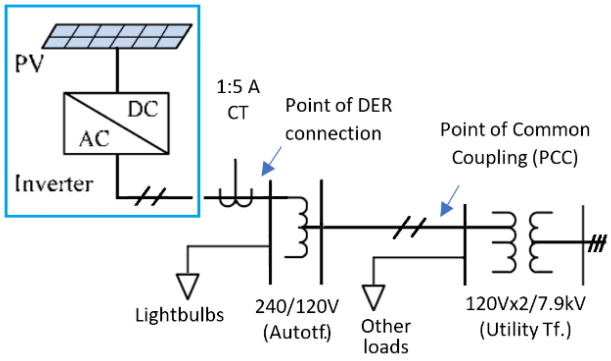

Figure C.2: Simplified diagram of the grid interconnection

Conditions:

Utility Transformer = 5 kVA. Inominal at PCC = $5x10^3/(120x2)$ = 20.83A.

Consider Max load is 48.4% Imax at PCC =10.08 A at 120V side (PCC)

= 5.04 at 240V side (Point of DER) = 0.97 A at CT

A) Load OFF, PV ON: All current from PV to the grid.

1. Lights OFF

2.18.18, clear morning.

Table C.16: Experimental results for RMS current C

A RMS	Percentage (%) of Imax						
I Fund	I Fund	C I 3	C I 5	C I 7	C I 9	C I 11	C I 13
0.76	77.83	6.34	5.17	3.08	2.97	2.57	2.88
0.76	78.37	6.42	5.22	3.09	2.90	2.59	2.84
0.76	78.45	6.37	5.20	3.07	2.99	2.61	2.85
0.76	78.36	6.34	5.24	3.08	3.03	2.64	2.89

2. Lights ON

2.18.18, Clear morning

Table C.17: Experimental results for RMS current C

A RMS	Percentage (%) of Imax						
I Fund	I Fund	C I 3	C I 5	C I 7	C I 9	C I 11	C I 13
0.79	81.64	6.59	5.32	3.14	3.03	2.71	2.85
0.80	82.30	6.47	5.12	3.04	2.98	2.66	2.82
0.80	82.10	6.31	5.12	3.12	3.07	2.75	2.87
0.80	82.61	6.40	5.08	3.10	3.03	2.72	2.87

11.20.17, Clear morning

Table C.18: Experimental results for RMS current C

A RMS	Percentage (%) of Imax						
Fund.	Fund.	C I 3	C I 5	C I 7	C I 9	C I 11	C I 13
0.69	71.36	6.21	4.91	3.44	3.27	2.71	3.17
0.66	68.07	5.70	4.60	3.34	3.24	2.74	3.15
0.72	73.80	6.19	4.86	3.48	3.37	2.88	3.19
0.72	73.76	6.27	4.89	3.53	3.31	2.82	3.12
0.71	73.35	6.21	4.69	3.56	3.41	2.86	3.28

B) Load On, PV Off. Only grid feeds load.

Lights OFF

2.18.18, clear morning

Table C.19: Experimental results for RMS current C

A RMS	Percentage (%) of Imax						
I Fund	I Fund	C I 3	C I 5	C I 7	C I 9	C I 11	C I 13
0.99	102	0.53	1.30	1.42	0.85	1.08	1.46
0.99	102	0.54	1.31	1.44	0.85	1.08	1.47
0.99	102	0.52	1.30	1.44	0.85	1.07	1.46
0.99	102	0.53	1.30	1.45	0.86	1.08	1.46

Lights ON

2.18.18, clear morning

Table C.20: Experimental results for RMS current C

A RMS	Percentage (%) of Imax						
I Fund	I Fund	C I 3	C I 5	C I 7	C I 9	C I 11	C I 13
0.99	102	0.52	1.29	1.44	0.85	1.08	1.43
0.99	102	0.55	1.28	1.44	0.85	1.08	1.43
0.99	102	0.51	1.29	1.45	0.86	1.10	1.45
0.99	102	0.53	1.28	1.44	0.85	1.09	1.45

2.18.18, clear morning

Table C.21: Experimental results for RMS current C

A RMS	Percentage (%) of Imax						
I Fund	I Fund	C I 3	C I 5	C I 7	C I 9	C I 11	C I 13
0.99	102	0.52	1.32	1.45	0.84	1.10	1.46
0.99	102	0.55	1.31	1.45	0.87	1.11	1.46
0.99	102	0.52	1.30	1.44	0.86	1.10	1.48
0.99	102	0.52	1.30	1.42	0.84	1.11	1.46

2.18.18, clear morning

Table C.22: Experimental results for RMS current C

A RMS	Percentage (%) of Imax						
I Fund	I Fund	C I 3	C I 5	C I 7	C I 9	C I 11	C I 13
0.99	100	0.51	1.32	1.43	0.85	1.11	1.46
0.99	100	0.52	1.30	1.44	0.84	1.11	1.45
0.99	100	0.53	1.29	1.44	0.86	1.11	1.46
0.99	100	0.52	1.32	1.43	0.85	1.09	1.45

2.16.18, overcast afternoon

Table C.23: Experimental results for RMS current C

A RMS	Percentage (%) of Imax						
I Fund	I Fund	C I 3	C I 5	C I 7	C I 9	C I 11	C I 13
0.99	102	0.83	1.79	1.52	1.11	1.26	1.51
0.99	102	0.80	1.76	1.51	1.15	1.27	1.65
0.99	102	0.85	1.75	1.56	1.07	1.20	1.49
0.99	102	0.75	1.67	1.48	1.07	1.28	1.67

11.14.18, clear afternoon

Table C.24: Experimental results for RMS current C

A RMS	Percentage (%) of Imax						
I Fund.	I Fund.	C I 3	C I 5	C I 7	C I 9	C I 11	C I 13
0.96	99	1.75	2.13	3.31	2.65	3.23	3.77
0.97	99	1.64	2.16	3.18	2.68	3.09	3.69
0.97	100	1.58	2.09	3.18	2.73	3.05	3.71
0.97	100	1.56	2.11	3.22	2.76	2.98	3.64
0.98	101	1.30	2.04	3.15	2.77	3.18	3.91

C) Current from grid and PV. Load ON, PV ON.

Current A

Lights OFF

2.18.18, clear morning

Table C.25: Experimental results for RMS current A

A RMS	Percentage (%) of Imax						
I Fund	I Fund	A I 3	A I 5	A I 7	A I 9	A I 11	A I 13
0.74	76	2.14	2.67	2.94	1.27	2.04	2.37
0.74	77	2.12	2.68	2.98	1.25	2.04	2.33
0.74	77	2.17	2.73	2.95	1.20	2.06	2.35
0.75	77	2.21	2.68	3.01	1.33	2.03	2.42

Lights ON

2.18.18, clear morning

Table C.26: Experimental results for RMS current A

A RMS	Percentage (%) of Imax						
I Fund	I Fund	A I 3	A I 5	A I 7	A I 9	A I 11	A I 13
0.75	78	2.06	2.71	2.97	1.19	2.12	2.34
0.76	78	2.10	2.61	3.00	1.30	2.05	2.39
0.76	78	2.24	2.63	3.09	1.41	2.02	2.46
0.77	80	2.29	2.56	3.05	1.50	1.96	2.38

11.20.17, clear morning

Table C.27: Experimental results for RMS current A

A RMS	Percentage (%) of Imax						
I Fund.	I Fund.	A I 3	A I 5	A I 7	A I 9	A I 11	A I 13
0.70	72	4.75	3.75	3.18	3.06	2.40	2.91
0.72	74	4.91	3.86	3.23	3.06	2.59	2.98
0.71	73	4.57	3.57	3.35	2.91	2.29	2.90
0.73	75	4.67	3.64	3.36	2.94	2.26	2.85
0.74	76	4.91	3.83	3.33	3.11	2.43	2.84

Current C

Lights OFF

2.8.17, clear morning

Table C.28: Experimental results for RMS current C

A RMS	Percentage (%) of Imax						
I Fund	I Fund	C I 3	C I 5	C I 7	C I 9	C I 11	C I 13
0.90	93	2.12	2.14	2.59	2.39	2.99	3.13
0.91	94	2.07	2.14	2.60	2.42	3.04	3.14
0.91	94	2.01	2.09	2.59	2.42	2.95	3.12
0.91	94	2.06	2.13	2.51	2.42	2.95	3.14
0.91	94	2.02	2.09	2.58	2.42	2.96	3.06

2.16.18, clear morning

Table C.29: Experimental results for RMS current C

A RMS	Percentage (%) of Imax						
I Fund	I Fund	C I 3	C I 5	C I 7	C I 9	C I 11	C I 13
0.75	77	3.04	3.17	3.61	2.87	2.65	3.17
0.73	75	3.11	3.44	3.58	2.99	2.56	3.03
0.78	81	2.93	3.13	3.32	3.08	2.81	3.47

Lights ON

2.16.18, clear morning

Table C.30: Experimental results for RMS current C

A RMS	Percentage (%) of Imax						
I Fund	I Fund	C I 3	C I 5	C I 7	C I 9	C I 11	C I 13
0.76	78	2.97	3.32	3.66	2.94	2.45	3.05
0.72	74	3.20	3.46	3.68	3.03	2.66	3.26
0.72	74	3.14	3.55	3.56	3.10	2.80	3.65
0.76	78	2.94	3.27	3.57	2.96	2.56	3.57

Reference conditions for the minimum acceptable case

Out of the previous conditions, the worst cases detected are

Table C.31: Experimental results for RMS current C

C I 3	C I 5	C I 7	C I 9	C I 11	C I 13	I rated, CT
5.78	3.58	2.16	2.31	1.98	2.33	0.9708
4	4	4	4	2	2	x1

That means we would need at least the following currents to comply in each case

Table C.32: Experimental results for RMS current C

	Max. Harmonic detected, A RMS					
	C I 3	C I 5	C I 7	C I 9	C I 11	C I 13
Max. Harm.	0.06	0.03	0.02	0.02	0.02	0.02
Min. Imax	1.40	0.87	0.52	0.56	0.96	1.13

Out of those, the highest is 1.40 A RMS at the CT side, which corresponds to 7.28 A RMS at the point of DER connection.

Connecting this system to anything above such limit is acceptable.

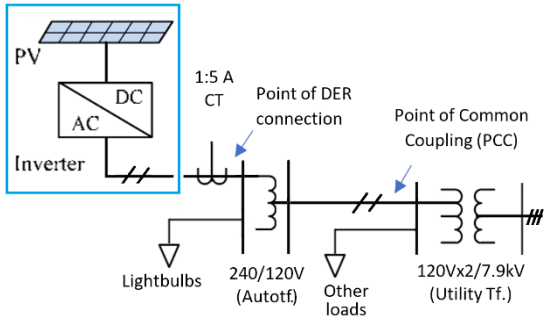

Figure C.3: Simplified diagram of the grid interconnection

Conditions:

Imax at PCC =14.56 A at 120V side (PCC) = 7.28 at 240V side (Point of DER) = 1.40 A at CT

Consider Max load 70%. Inominal at PCC: VxI= (120x2)x(14.56x1/0.70) = 5 kVA Minimum for resistive loads.

REFERENCES

[1] U.S. Energy Information Administration, "Independent Statistics & Analysis," 16 February 2017. [Online]. Available: https://www.eia.gov/tools/faqs/faq.php?id=105&t=3.

[2] M. Green, Operating principles technology and System Applications. Chapter 1, Kensington: University of New South Wales., 1998.

[3] A. Rohatgi, *ECE 6453 - Solar cells. Chapter 1B,* Georgia Tech, Fall 2016.

[4] A. Rohatgi, *ECE 6453 - Solar cells. Chapter 11,* Georgia Tech, Fall 2016.

[5] M. Green, *Solar Cells, Operating principles technology and System Applications. Chapter 4.,* Kensington: University of New South Wales., 1998.

[6] J. Peças Lopes, N. Hatziargyriou, J. Mutale, P. Djapic and N. Jenkins, "Integrating distributed generation into electric power systems: A review of drivers, challenges and opportunities," *Electric Power Systems Research,* vol. 77, no. July 2007.

[7] M. A. Mahmud, M. J. Hossain and H. R. Pota, "Analysis of Voltage Rise Effect on Distribution Network with Distributed Generation.".

[8] N. Jenkins, J. Ekanayake and G. Strbac, Distributed Generation. IET Renewable Energy series 1., London: The Institution of Engineering and Technology, 2010.

[9] U.S. Department of Energy - Office of Electricity Delivery and Energy Reliability., "Summary Report: DOE Microgrid Workshop," 2012.

[10] Office of Electricity Delivery, *DOE Microgrid Workshop,* San Diego, California, August 30-31, 2011.

[11] S. Parhizi, H. Lotfi, A. Khodaei and S. Bahrramirad, "State of the Art in Research on Microgrids: A Review".*IEEE Access 3:1-1.*

[12] D. Quiggin, S. Cornell, M. Tierney and R. Buswell, "A simulation and optimisation study: Towards a decentralised microgrid, using real world fluctuation data," *Energy,* vol. 41, pp. 549-559, 2012.

[13] A. Khodaei, "Provisional microgrids," *IEEE Trans. Smart Grid,* vol. 6, no. 3, p. 1107–1115, May 2015.

[14] A. Mohamed, V. Salehi and O. Mohammed, "Real-time energy management algorithm for mitigation of pulse loads in hybrid microgrids," *IEEE Trans. Smart Grid,* vol. 3, p. 1911–1922, Dec. 2012..

[15] R. Pawelek, I. Wasiak, P. Gburczyk and R. Mienski, "Study on operation of energy storage in electrical power microgrid—Modeling and simulation, pp. 1–5.," in *14th Int. Conf. Harmon. Quality Power (ICHQP),* Sep. 2010.

[16] R. Yokoyama, T. Niimura and N. Saito, "Modeling and evaluation of supply reliability of microgrids including PV and wind power," in *in Proc. IEEE Power Energy Soc. General Meeting-Convers. Del. Elect. Energy 21st Century, pp. 1–5,* Jul. 2008.

[17] B. Falahati, A. Kargarian and Y. Fu, "Timeframe capacity factor reliability model for isolated microgrids with renewable energy resources," in *IEEE Power Energy Soc. General Meeting, pp. 1–8,* Jul. 2012.

[18] P. P. Varaiya, F. F. Wu and J. W. Bialek, "'Smart operation of smart grid: Risk-limiting dispatch," in *IEEE, vol. 99, no. 1, pp. 40–57,* Jan. 2011.

[19] M. Jun and A. J. Markel, "Simulation and analysis of vehicle-to-grid operations in microgrid," in *IEEE Power Energy Soc. General Meeting, pp. 1–5.,* Jul. 2012.

[20] R. Arghandeh, M. Pipattanasomporn and S. Rahman, "Flywheel energy storage systems for ride-through applications in a facility microgrid," *IEEE Trans. Smart Grid,* vol. 3, no. 4, pp. 1955-1962, Dec. 2012.

[21] H. e. a. Qi, "A resilient real-time system design for a secure and reconfigurable power grid," *IEEE Trans. Smart Grid,* vol. 2, no. 4, p. 770–781, Dec. 2011..

[22] F. Wang, J. Duarte and M. A. M. Hendrix, "Grid-interfacing converter systems with enhanced voltage quality for microgrid application - Concept and implementation," *IEEE Trans. Power Electron,* vol. 26, no. 12, p. 3501–3513, Dec. 2011.

[23] Y. W. Li, D. M. Vilathgamuwa and P. C. Loh, "A grid-interfacing power quality compensator for three-phase three-wire microgrid applications," *IEEE Trans. Power Electron,* vol. 21, no. 4, pp. 1021-1031, Jul. 2006.

[24] T. Lee and P. Cheng, "Design of a new cooperative harmonic filtering strategy for distributed generation interface converters in an islanding network," *IEEE Trans. Power Electron,* vol. 22, no. 5, p. 1919–1927, Sep. 2007.

[25] J. F. G. Cobben, W. L. Kling and J. M. A. Myrzik, "Power quality aspects of a future micro grid," in *Int. Conf. Future Power Syst., pp. 1–5.,* Nov. 2005.

[26] S. Chattopadhyay, M. Mitra and S. Sengupta, "Electric Power Quality. Chapter 2," Springer, 2011.

[27] S. Chattopadhyay, M. Mitra and S. Sengupta, Electric Power Quality. Chapter 4., 2011: Springer.

[28] IEEE Standards Association, *IEEE Std 519-2014. Recommended Practice and Requirements for Harmonic Control in Electric Power Systems.,* IEEE Power and Energy Society.

[29] International Electrotechnical Commission, *Electromagnetic compatibility (EMC). Part 4-7. Testing and measurement techniques.,* 2002: IEC.

[30] IEEE Standards Association, *IEEE Std 1547-2014. Standard for Interconnecting Distributed Resources with Electric Power Systems.,* IEEE Power and Energy Society.

[31] *American National Standard for Electric Power Systems and Equipment - Voltage Ratings (60 Hz),* The Association of Electrical Equipment and Medical Imaging Manufacturers.

[32] PG&E, "Voltage Regulation," 1999. [Online]. [Accessed 2016].

[33] Solartech Power, Inc, *N-Series 130W PV Module SPM130P-S-N.*

[34] Sputnik Engineering AG, *SolarMax 2000S/3000S/4200S/6000S Instruction Manual,* Biel/Bienne, Switzerland, 2008.

[35] A. Umana, *Module-level autonomous seting-less protection and monitoring of standalone and grid connected photovoltaic array systems using quadratic integration modeling, Ph.D. Dissertation,* Georgia Institute of Technology, School of Electrical and Computer Engineering, Atlanta, GA, 2015.

[36] Ecom Electronics, "Genesis 12V 24Ah Battery," [Online]. Available: https://www.ecomelectronics.com/p3391467/genesis-12v-24ah-battery-replacement-for-yuasa-np24-12b.html. [Accessed 2017].

[37] AcuAMP, *DC Current Switches and Transducers,* 2016.

[38] CR Magnetics, *Commercial and Metering Class Current Transformers,* St. Louis, MO, 2017.

[39] National Instruments, "Connecting Analog Voltage Signals to a DAQ Device," [Online]. Available: http://www.ni.com/getting-started/set-up-hardware/data-acquisition/analog-voltage. [Accessed 2017 June].

[40] National Instruments, *DAQ X Series. X Series User Manual NI 632x/634x/635x/636x Devices. NI USBX6163 Manual.*, 2010.

[41] Arbiter Systems, *Model 1133A Power Sentinel. Operation Manual.*, Paso Robles, CA.

[42] S. Chattopadhyay, M. Mitra and S. Sengupta, "Electric Power Quality," Springer, 2011, p. Chapter 2.

[43] J. Swingler, Reliability Characterisation of Electrical and Electronic Systems, Woodhead Publishing, 2015.

[44] National Instruments, "How To Measure Voltage," 11 May 2016. [Online]. Available: http://www.ni.com/tutorial/7113/en/. [Accessed June 2017].

[45] National Instruments, "Pinout Terminology and Definitions for NI DAQ Devices," August 2016. [Online]. Available: http://digital.ni.com/public.nsf/allkb/B478F1BC6556FA2F862571C0007E6062. [Accessed May 2017].

[46] IEEE Standards Association, "IEEE Std 519-2014. Recommended Practice and Requirements for Harmonic Control in Electric Power Systems.," IEEE Power and Energy Society, 2014.

[47] IEC, "IEC 61000-4-7:2002(E) Testing and measurement techniques - General guide on harmonics and interharmonics measurements and instrumentation, for power supply systems and equipment connected thereto," 2002.

[48] Pacific Gas & Electric Company, "Voltage Tolerance Boundary," 1999.